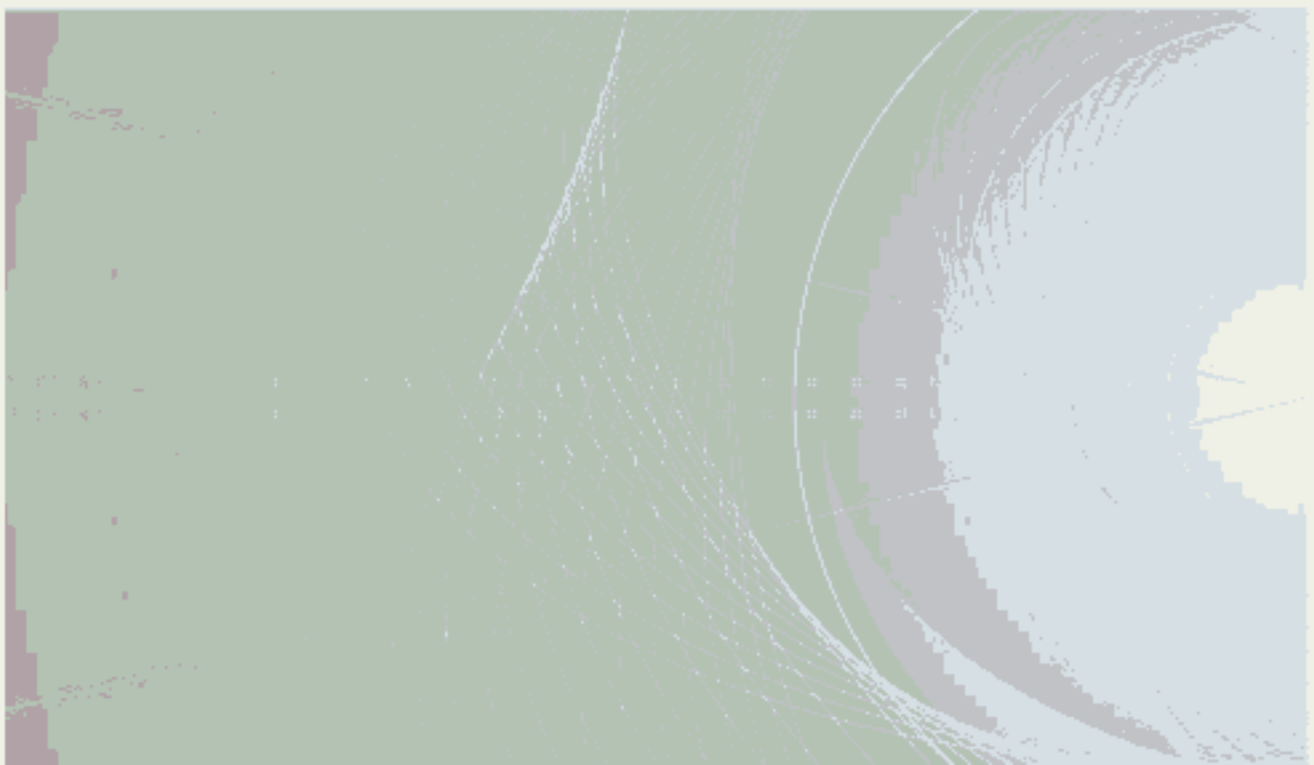


TECHNICAL REPORT



Derisking photovoltaic modules – Sequential and combined accelerated stress testing





THIS PUBLICATION IS COPYRIGHT PROTECTED
Copyright © 2020 IEC, Geneva, Switzerland

All rights reserved. Unless otherwise specified, no part of this publication may be reproduced or utilized in any form or by any means, electronic or mechanical, including photocopying and microfilm, without permission in writing from either IEC or IEC's member National Committee in the country of the requester. If you have any questions about IEC copyright or have an enquiry about obtaining additional rights to this publication, please contact the address below or your local IEC member National Committee for further information.

IEC Central Office
3, rue de Varembe
CH-1211 Geneva 20
Switzerland

Tel.: +41 22 919 02 11
info@iec.ch
www.iec.ch

About the IEC

The International Electrotechnical Commission (IEC) is the leading global organization that prepares and publishes International Standards for all electrical, electronic and related technologies.

About IEC publications

The technical content of IEC publications is kept under constant review by the IEC. Please make sure that you have the latest edition, a corrigendum or an amendment might have been published.

IEC publications search - webstore.iec.ch/advsearchform

The advanced search enables to find IEC publications by a variety of criteria (reference number, text, technical committee,...). It also gives information on projects, replaced and withdrawn publications.

IEC Just Published - webstore.iec.ch/justpublished

Stay up to date on all new IEC publications. Just Published details all new publications released. Available online and once a month by email.

IEC Customer Service Centre - webstore.iec.ch/csc

If you wish to give us your feedback on this publication or need further assistance, please contact the Customer Service Centre: sales@iec.ch.

Electropedia - www.electropedia.org

The world's leading online dictionary on electrotechnology, containing more than 22 000 terminological entries in English and French, with equivalent terms in 16 additional languages. Also known as the International Electrotechnical Vocabulary (IEV) online.

IEC Glossary - std.iec.ch/glossary

67 000 electrotechnical terminology entries in English and French extracted from the Terms and Definitions clause of IEC publications issued since 2002. Some entries have been collected from earlier publications of IEC TC 37, 77, 86 and CISPR.



IEC TR 63279

Edition 1.0 2020-08

TECHNICAL REPORT



Derisking photovoltaic modules – Sequential and combined accelerated stress testing

INTERNATIONAL
ELECTROTECHNICAL
COMMISSION

ICS 27.160

ISBN 978-2-8322-8737-8

Warning! Make sure that you obtained this publication from an authorized distributor.

CONTENTS

FOREWORD	5
1 Scope	7
2 Normative references	7
3 Terms and definitions	8
4 Framework for sequential and combined stress testing	8
5 Sequential and cyclic sequential test methods	9
5.1 Extended damp heat and addition of ultraviolet light	9
5.2 Sequential/combined testing with damp-heat, thermal cycling and ultraviolet light	10
5.3 Consideration of interaction of UV radiation and damp heat	12
5.4 Test-to-failure—A sequential test protocol	13
5.5 Sequential test protocol optimized for differentiating backsheets	16
5.6 Mechanical stress testing in combination with damp-heat, humidity-freeze, and thermal-cycling tests for examining cell cracking and its effects	20
6 Mechanism-specific multi-factor stress tests	22
6.1 General	22
6.2 Testing for delamination	22
6.2.1 General	22
6.2.2 Delamination – UV irradiation with high-temperature stress	22
6.2.3 Delamination – UV irradiation with thermal-cycling stress and humidity freeze	23
6.2.4 Delamination – UV irradiation with cyclic dynamic mechanical loading, thermal cycling stress, and humidity freeze	24
6.2.5 Delamination – Temperature, humidity, and electric field associated with system voltage	25
6.3 Testing for potential-induced degradation	28
6.3.1 General	28
6.3.2 Testing for potential-induced degradation with humidity, voltage, bias, and light	28
6.3.3 Factor of salt mist	29
6.4 Testing in damp heat with current injection and as a function of temperature	30
6.5 Cell cracking and propagation in cyclic loading at various temperatures.....	31
7 Combined-accelerated stress testing	33
7.1 Combined-accelerated stress testing for tropical environments	33
7.2 Combined-accelerated stress testing for multiple environments	36
8 Future directions.....	39
Annex A (informative) Overview of degradation modes and causal stress factors	41
Annex B (informative) Failure modes plotted on a failure tree diagram for selected clauses in this document	43
Annex C (informative) Summary table of sequential and combined testing: Samples, factors, combination, and stress-test results	44
Bibliography	49
Figure 1 – Framework for sequential and combined stress testing, showing three axes of comprehensiveness – testing samples, the number of stress factors of the natural environment, and their sequence or combination of application.	9
Figure 2 – Fraction power loss of modules though stress testing	10

Figure 3 – (a) Combined test sequence, and resulting (b) normalized power loss, (c) short-circuit current (I_{SC}), and (d) fill factor (FF) [1]	11
Figure 4 – Power degradation of modules in 85 °C and 85 % relative humidity as a function of extent of preconditioning under Xe light [9]	13
Figure 5 – (a) Overview of the test-to-failure sequences, and (b) results showing module power normalized to their post-light-soak values for seven module types.....	14
Figure 6 – Examples of field-relevant degradation modes seen in modules tested in the test-to-failure protocol	15
Figure 7 – Module accelerated sequential tests (MAST)	17
Figure 8 – Degradation modes from MAST and fielded modules	19
Figure 9 – (a) Front-side mini-module exposure in a xenon weathering chamber with water spray; (b) fielded module with six years of service in North America with 30 % power loss [21]	20
Figure 10 – (a) Test-stage description; (b) relative change in standard test condition (STC) module parameters as a function of stage and maximum power determined at STC [23]	21
Figure 11 – (a) Stress testing at 65 °C combined with UV radiation dose of 180 W/m in the range of 300–400 nm, 900 h; (b) 75 °C without UV radiation, 1 000 h [28]	23
Figure 12 – Delamination in sequential test	25
Figure 13 – Delamination associated with system voltage	27
Figure 14 – Degradation of three modules with and without UV-A light irradiance in chamber at 60 °C, 85 % RH, and 1 000 V (positive or negative polarity depending on the sample)	29
Figure 15 – Sheet resistance measured on glass surfaces with various soil types, as a function of relative humidity (RH %), at 60 °C [41]	30
Figure 16 – Cyclic unidirectional 4-point bending with loading alternating between 0 N and 500 N at different temperatures as shown, with duration of 4 s at each of the high- and low-pressure dwells, 10 000 to 30 000 cycles with pressure (“Press”) from the front-glass side or backsheets side [49]	32
Figure 17 – Example of 24 h PV module combined accelerated stress-testing protocol modified from ASTM D7869	34
Figure 18 – Shrinkage of polymer C backsheets leading to delamination and cracking	35
Figure 19 – Multiple-environment C-AST sequence	37
Figure 20 – Failure of two mini-modules with a polymer B outer-layer backsheets type undergoing different multiple-environment C-AST sequences	38
Table 1 – Extended damp heat and ultraviolet light	10
Table 2 – Sequential/combined testing with damp-heat thermal cycling and ultraviolet radiation	12
Table 3 – Ultraviolet light and damp-heat interaction	13
Table 4 – Test-to-failure – Sequential test protocol	16
Table 5 – Module accelerated stress test 1 (MAST #1)	18
Table 6 – Module accelerated stress test 2 (MAST #2)	18
Table 7 – Module accelerated stress test 3 (MAST #3)	18
Table 8 – SML-TC-HF sequential test	21
Table 9 – UV irradiation under high-temperature conditions	23
Table 10 – UV irradiation with TC stress	24
Table 11 – UV irradiation with DML-TC-HF sequential test	25

Table 12 – DH – Negative system bias stress sequential test	28
Table 13 – UV irradiation – negative system bias stress combined test	29
Table 14 – Bending load test at various temperatures	33
Table 15 – Partial list of observed degradation modes, attributed mechanisms, and stress factors seen in the first application of the combined accelerated stress-testing protocol based on ASTM D7869	35
Table 16 – Combined-accelerated stress test (Tropical 24 h ASTM D7869-based sequence)	36
Table 17 – Multiple-environment combined-accelerated stress test	38
Table A.1 – Degradation modes and potential stress factors that can lead to their manifestation	42
Table C.1 – Table summarizing sequential and combined stress testing	44

INTERNATIONAL ELECTROTECHNICAL COMMISSION

**DERISKING PHOTOVOLTAIC MODULES – SEQUENTIAL
AND COMBINED ACCELERATED STRESS TESTING**

FOREWORD

- 1) The International Electrotechnical Commission (IEC) is a worldwide organization for standardization comprising all national electrotechnical committees (IEC National Committees). The object of IEC is to promote international co-operation on all questions concerning standardization in the electrical and electronic fields. To this end and in addition to other activities, IEC publishes International Standards, Technical Specifications, Technical Reports, Publicly Available Specifications (PAS) and Guides (hereafter referred to as "IEC Publication(s)"). Their preparation is entrusted to technical committees; any IEC National Committee interested in the subject dealt with may participate in this preparatory work. International, governmental and non-governmental organizations liaising with the IEC also participate in this preparation. IEC collaborates closely with the International Organization for Standardization (ISO) in accordance with conditions determined by agreement between the two organizations.
- 2) The formal decisions or agreements of IEC on technical matters express, as nearly as possible, an international consensus of opinion on the relevant subjects since each technical committee has representation from all interested IEC National Committees.
- 3) IEC Publications have the form of recommendations for international use and are accepted by IEC National Committees in that sense. While all reasonable efforts are made to ensure that the technical content of IEC Publications is accurate, IEC cannot be held responsible for the way in which they are used or for any misinterpretation by any end user.
- 4) In order to promote international uniformity, IEC National Committees undertake to apply IEC Publications transparently to the maximum extent possible in their national and regional publications. Any divergence between any IEC Publication and the corresponding national or regional publication shall be clearly indicated in the latter.
- 5) IEC itself does not provide any attestation of conformity. Independent certification bodies provide conformity assessment services and, in some areas, access to IEC marks of conformity. IEC is not responsible for any services carried out by independent certification bodies.
- 6) All users should ensure that they have the latest edition of this publication.
- 7) No liability shall attach to IEC or its directors, employees, servants or agents including individual experts and members of its technical committees and IEC National Committees for any personal injury, property damage or other damage of any nature whatsoever, whether direct or indirect, or for costs (including legal fees) and expenses arising out of the publication, use of, or reliance upon, this IEC Publication or any other IEC Publications.
- 8) Attention is drawn to the Normative references cited in this publication. Use of the referenced publications is indispensable for the correct application of this publication.
- 9) Attention is drawn to the possibility that some of the elements of this IEC Publication may be the subject of patent rights. IEC shall not be held responsible for identifying any or all such patent rights.

The main task of IEC technical committees is to prepare International Standards. However, a technical committee may propose the publication of a technical report when it has collected data of a different kind from that which is normally published as an International Standard, for example "state of the art".

IEC TR 63279, which is a Technical Report, has been prepared by IEC technical committee 82: Solar photovoltaic energy systems.

The text of this Technical Report is based on the following documents:

Enquiry draft	Report on voting
82/1657/DTR	82/1692B/RVDTR

Full information on the voting for the approval of this technical report can be found in the report on voting indicated in the above table.

This document has been drafted in accordance with the ISO/IEC Directives, Part 2.

The committee has decided that the contents of this document will remain unchanged until the stability date indicated on the IEC website under "<http://webstore.iec.ch>" in the data related to the specific document. At this date, the document will be

- reconfirmed,
- withdrawn,
- replaced by a revised edition, or
- amended.

IMPORTANT – The 'colour inside' logo on the cover page of this publication indicates that it contains colours which are considered to be useful for the correct understanding of its contents. Users should therefore print this document using a colour printer.

DERISKING PHOTOVOLTAIC MODULES – SEQUENTIAL AND COMBINED ACCELERATED STRESS TESTING

1 Scope

This document reviews research into sequential and combined accelerated stress tests that have been devised to determine the potential for degradation modes in PV modules that occur in the field that single-factor and steady-state tests do not show. This document is intended to provide data and theory-based motivation and help visualize the next steps for improved accelerated stress tests that will derisk PV module materials and designs. Any incremental savings as a result of increased reliability and reduced risk translates into lower levelized cost of electricity for PV. Lower costs will result in faster adoption of PV and the associated benefits of renewable energy.

2 Normative references

The following documents are referred in the text in such a way that some or all of their content constitutes requirements of this document. For dated references, only the edition cited applies. For undated references, the latest edition of the referenced document (including any amendments) applies.

IEC 60721-2-1, *Classification of environmental conditions – Part 2-1: Environmental conditions appearing in nature – Temperature and humidity*

IEC 61215-1:2016, *Terrestrial photovoltaic (PV) modules – Design qualification and type approval – Part 1: Test requirements*

IEC 61215-2:2016, *Terrestrial photovoltaic (PV) modules – Design qualification and type approval – Part 2: Test procedures*

IEC 61730-2:2016, *Photovoltaic (PV) module safety qualification – Part 2: Requirements for testing*

IEC TS 61836, *Solar photovoltaic energy systems – Terms, definitions and symbols*

IEC TS 62782:2016, *Photovoltaic (PV) modules – Cyclic (dynamic) mechanical load testing*

IEC 62788 (all parts), *Measurement procedures for materials used in photovoltaic modules*

IEC TS 62804-1, *Photovoltaic (PV) modules – Test methods for the detection of potential-induced degradation – Part 1: Crystalline silicon*

IEC TS 62804-1-1, *Photovoltaic (PV) modules – Test methods for the detection of potential-induced degradation – Part 1-1: Crystalline silicon – Delamination*

ASTM D7869-17 *Standard Practice for Xenon Arc Exposure Test with Enhanced Light and Water Exposure for Transportation Coatings*

3 Terms and definitions

For the purposes of this document, the terms and definitions given in IEC TS 61836 apply.

ISO and IEC maintain terminological databases for use in standardization at the following addresses:

- IEC Electropedia: available at <http://www.electropedia.org/>
- ISO Online browsing platform: available at <http://www.iso.org/obp>

4 Framework for sequential and combined stress testing

A number of researchers, companies and testing laboratories have explored aspects of sequential and combined stress testing to fill outstanding needs. Such needs include testing beyond IEC 61215-2, which for the most part does not purport to examine for end-of-life wear-out and failure mechanisms. In other cases, stresses are sequenced and combined to elicit failure modes that have been seen in the field that existing IEC tests may not evaluate.

A framework for organization is proposed that implements stress factors of the natural environment, sequences and combinations of applying them, and sample types that may be employed for evaluation. To illustrate this, Figure 1 is introduced, which gives a three-dimensional plot with the axes of sample, factor, and combination, that together indicate the comprehensiveness of test methods to represent the effects of the natural environment on the sample in accelerated testing.

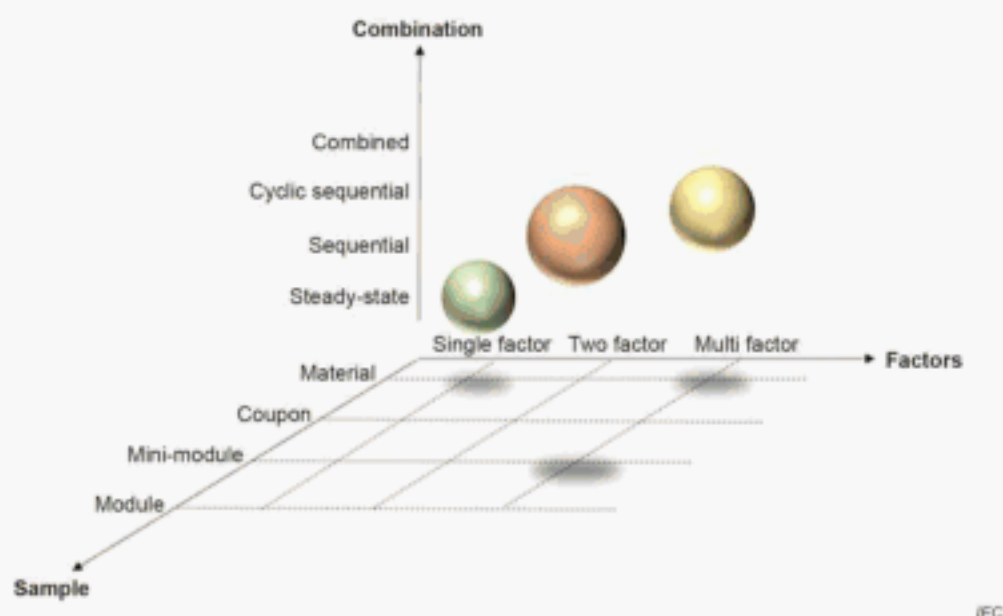
First the sample comprehensiveness axis of Figure 1 is discussed. As a new material is explored, the material itself is studied to achieve a basic understanding of its intrinsic degradation mechanisms and durability. Thus, material and coupon tests as they are performed now according to IEC 62788 series material tests will be valuable. However, failures often occur at the interfaces between materials, and the performance of one component of the module often depends on the behaviour of another component or material in the assembly. Therefore, to represent the material interactions, boundary conditions in actual use, and stresses experienced, it is necessary to examine mini-modules, and most comprehensively, full-size modules with all their components.

Next the factors comprehensiveness axis is discussed. This is the number of stress factors of the natural environment applied in testing of the sample. Moving from single stress factor tests to multi-factor tests increases confidence of capturing the factors relevant to both known and unknown degradation modes. Using one factor alone may be useful to evaluate an acceleration factor or an activation energy associated with that stress for a specific degradation mode or mechanism that is already understood to depend principally on that stress factor independently of others.

Finally, the combination comprehensiveness axis is discussed. It represents the manner of integration of the stress factors on the sample. We seek to sequence and combine the stress factors in a manner that represents how they appear together in nature to increase the probability of accelerating only the real degradation modes in the module as they would manifest in nature. As stress factors are considered, individually or in combination, it is necessary to understand whether stress levels applied are maintained within the levels of the natural environment, or if they are exceeded. If exceeded, acceleration of the test may be increased, but there is significantly increased potential of incurring degradation modes that are artifacts—modes not necessarily representative of those that would be seen in the natural environment.

Tables are given in this document for various experimental results in the framework of Figure 1 condensed into two dimensions. These serve to explain how the sequential and combined accelerated stress tests, with consideration of sample type, factors, and their combination, have served to produce particular failures or degradation modes. In these condensed two-

dimensional plots, the various column-listed stress factors may be an individual stress factor such as mechanical load, or an existing IEC 61215 stress test, such as damp heat or thermal cycling, which in itself contains factors of temperature cycling and current through the cell circuit. Annexes in which the failure modes are collected for reference are as follows: Annex A : Overview of degradation modes and causal stress factors, Annex B: Failure modes plotted on a failure tree diagram for selected clauses in this document, and Annex C : Summary table of sequential and combined testing: samples, factors, combination, and stress test results of the samples studied. The templates in these Annexes may be useful for classifying other failure or degradation modes as they become understood in the future.



Points shown are possibilities for testing within this space.

Figure 1 – Framework for sequential and combined stress testing, showing three axes of comprehensiveness: testing samples, the number of stress factors of the natural environment, and their sequence or combination of application

5 Sequential and cyclic sequential test methods

5.1 Extended damp heat and addition of ultraviolet light

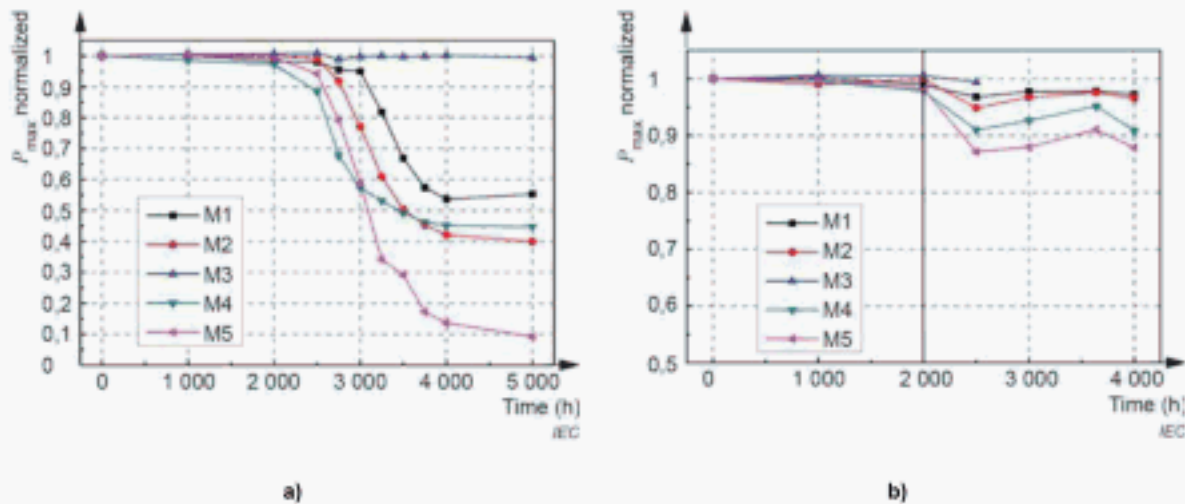
Extended damp-heat (DH) testing has frequently been used to attempt to differentiate durability of PV modules. An example of this is shown in Figure 2a). Five modules undergo five iterations of 1 000 h duration DH tests at 85 °C and 85 % relative humidity (RH). Four module types exhibit great degradation after 2 000 h that is due to fill factor (FF) loss from metallization to silicon contact-resistance increase. The degradation comes at test conditions with temperature in combination with humidity significantly exceeding those found for modules in PV field installations, and the degradation mechanisms observed with extended DH tests have frequently been inconsistent with those seen in fielded PV modules [1] 1. Reviews of agglomerated field-degradation data for crystalline silicon cell modules have shown degradation primarily by short-circuit current (I_{sc}) loss followed by FF loss and the least degradation exhibited by open-circuit voltage (V_{oc}) [2].

Excessive humidity may lead to unrealistically high levels of acetic acid formation, leading in turn to unrealistically high FF losses through grid finger to silicon contact corrosion and other mechanisms. Therefore, excessively long DH stress tests that produce very high acetic acid

1 Numbers in square brackets refer to the Bibliography.

levels are believed to have limited use in evaluating the durability of conventional crystalline silicon PV modules installed in the field.

If, after 2 000 h of DH testing, modules were transferred for ultraviolet (UV) exposure in a DH environment with an 85 °C target module temperature, then the power losses were more modest as shown in Figure 2b) and reported to be primarily associated with I_{sc} degradation [1], which is representative of what is observed in the field. Including UV radiation is necessary to represent this stress factor of the natural environment. A summary of the sample type used, stress factors, and their sequence and combination, along with resulting degradation modes seen for the modules in the study, is given in Table 1.



- a) Module M1 with thermoplastic and modules M2–M5 with ethylene vinyl acetate encapsulant through 1 000 h of 85 °C and 85 % relative humidity damp heat cycles;
- b) Modules through 2 000 h of the damp heat exposure in (a) followed by placement under UV radiation and damp heat [1].

Figure 2 – Fraction power loss of modules through stress testing

Table 1 – Extended damp heat and ultraviolet light

Sequential/ combined	Stress factor A	Stress factor B	Combined stress effect(s)
	DH	UV+DH	
Material			
Coupon			
Mini-Module			
Module	85 °C/85 % RH 2 000 h	200 W/m ² UV-A, 85 °C module temperature, 2 000 h	Degradation of I_{sc} and FF in better proportion to field, toward field-relevant levels of humidity after UV exposure.
Sequential / Combined: A B			

5.2 Sequential/combined testing with damp-heat, thermal cycling and ultraviolet light

A sequential test is shown in Figure 3a) developed for the application of additional stress factors with more balanced levels considering the relative levels seen in outdoor exposure and to produce degradation modes in reasonable proportion to those seen in the field. In addition to DH and DH with UV sequences, temperature cycling is included, which adds thermomechanical stresses. Table 2 summarizes the stress factors applied, the levels, and the results of the combined stress effects.

Because of acetic acid formation, attention has been given to humidity levels when alternating between DH in the dark, which drives humidity into the module, and DH with UV radiation, which drives moisture out of the module, as illumination does in PV modules installed in the field [1]. On the backsheet side of the cell, humidity levels reach correspondence with chamber equilibrium; on the front side of the cell, simulations show humidity levels stabilizing around 30 % lower in the alternating sequence than in the continuous DH case, reducing unrealistically high formation of acetic acid that can affect the metallization-silicon contact of some solar cells. The UV can also degrade the cell-front passivation, reducing I_{sc} and V_{oc} [3], and it can cause transmission loss in the encapsulant, contributing to degrading I_{sc} [4], which is observed in the results in Figure 3b) to d).

Appropriate humidity levels and durations for accelerated tests in DH depend on whether moisture-barrier components are required and on the degradation kinetics of the particular solar cells [5]. Based on simulations, it has been proposed that testing for more than 3 000 h in 85 °C and 85 % RH is necessary to duplicate the moisture-ingress distance experienced by an edge seal after 25 years of exposure in the Miami, Florida (USA) use environment [6]. This level, however, causes hydrolysis of polyethylene terephthalate (PET) layers in backsheets used in many crystalline silicon cell-based modules. Extensive degradation by hydrolysis of PET has not been seen in fielded PV modules, so extended DH testing (in this case, 85 °C, 85 % RH, and 3 000 h) is considered too extreme a level for testing failure modes that could be linked to PET degradation [7].

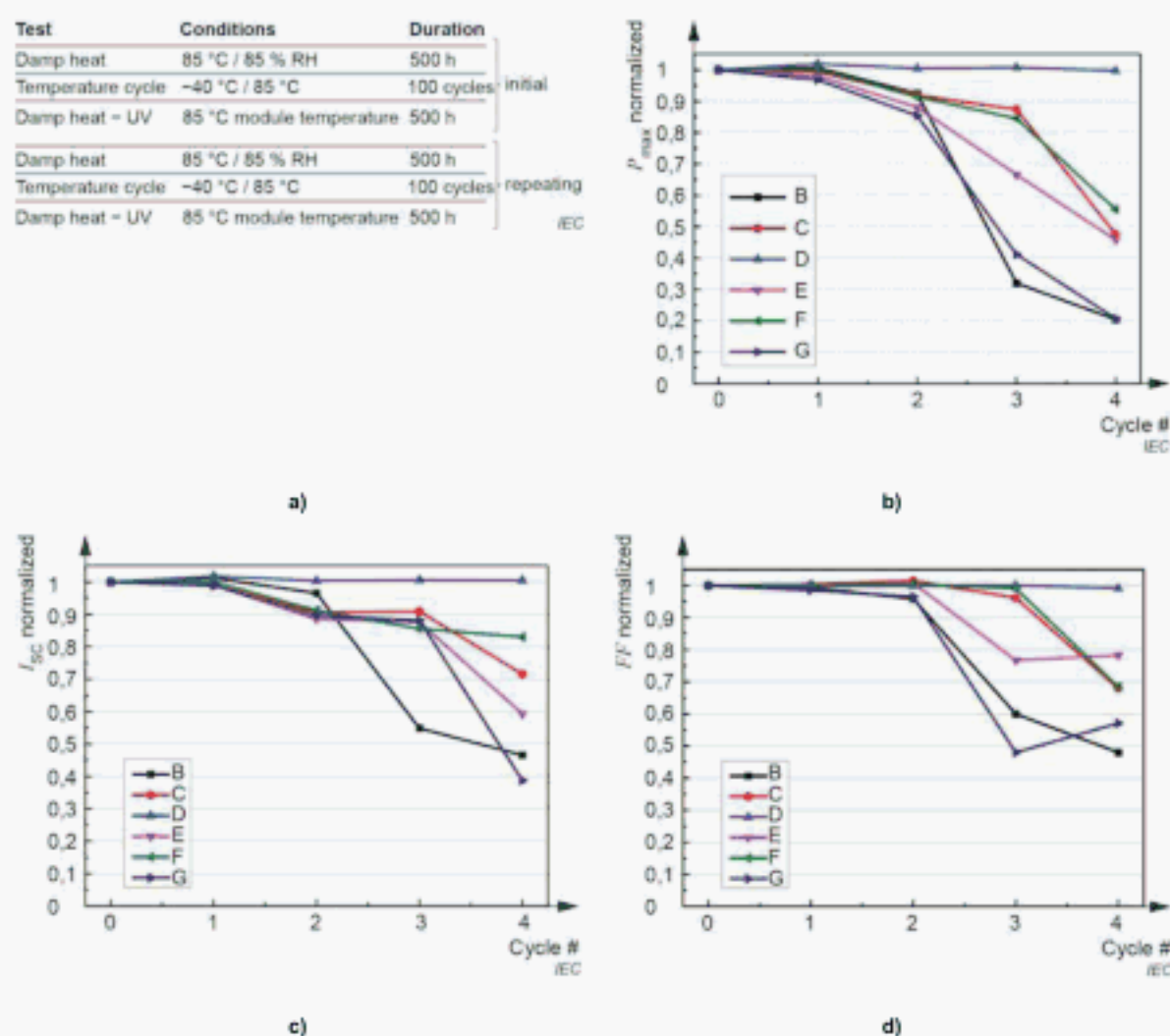
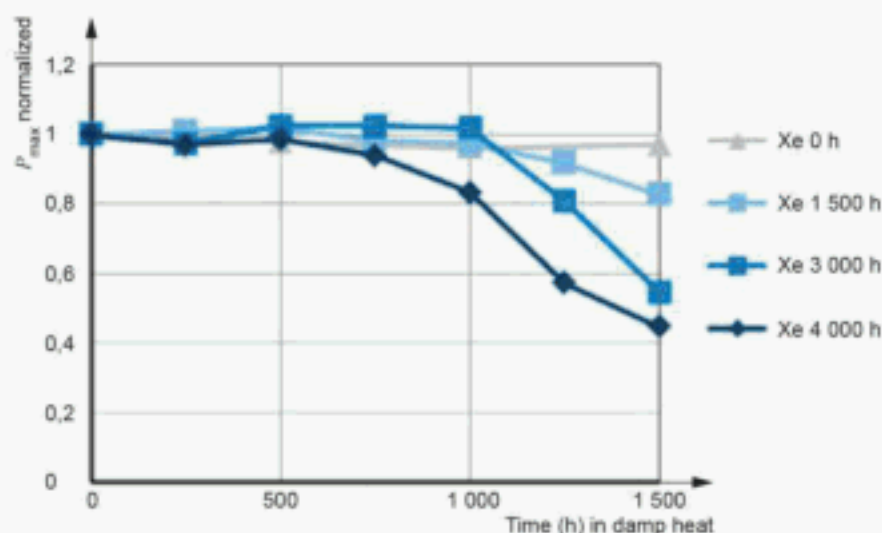


Figure 3 – a) Combined test sequence, and resulting b) normalized power loss, c) short-circuit current (I_{sc}), and d) fill factor (FF) [1]



IEC

Figure 4 – Power degradation of modules in 85 °C and 85 % relative humidity as a function of extent of preconditioning under Xe light [9]

Table 3 – Ultraviolet light and damp-heat interaction

Sequential/ combined	Stress factor A	Stress factor B	Combined stress effect(s)
	UV	DH	
Material			
Coupon			
Mini-module	90 W/m ² (300 nm to 400 nm), 90 °C module temperature 1 500 h to 4 000 h	85 °C/ 85 % RH 1 500 h	UV radiation activates appearance of acetic acid in subsequent DH, causing increased contact resistance of grid fingers to silicon
Module			
Sequential: A B			

5.4 Test-to-failure – A sequential test protocol

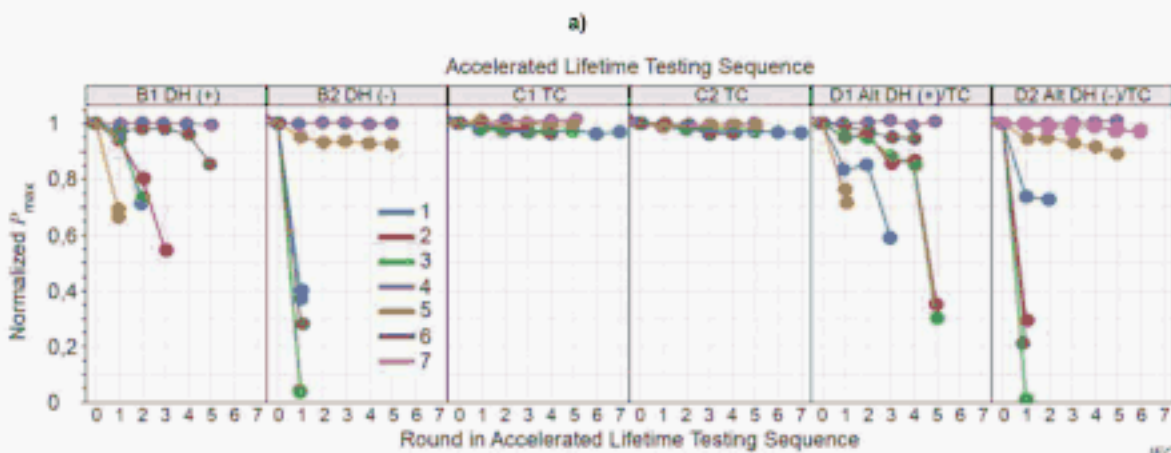
The "Terrestrial Photovoltaic Module Accelerated Test-to-Failure (TTF) Protocol" was devised in 2008 and subsequently demonstrated to fill a gap between qualification testing and comprehensive accelerated lifetime testing [10-12]. This protocol shown in Figure 5a) also adds stress sequences in combinations, which manifest in degradation mechanisms not presently examined in standardized qualification testing. The TTF protocol extends the environmental chamber testing until failure modes in the module can be seen to a sufficient magnitude to be studied (e.g. greater than 20 % degradation). The protocol was devised to compare the reliability of different modules on a quantitative basis and to evaluate the performance of new module types to incumbents. A key technical and intellectual exercise not to be overlooked in the analysis of the TTF results is an evaluation of the significance of degradation modes or failures seen. This is in part because the stress levels applied are far greater than found in nature, therefore spurious failures may occur. Field testing and further chamber testing to determine acceleration factors for issues found may need to be performed to evaluate if the degradation modes will be seen in fielded PV modules.

Examples of module power results through the TTF protocol are shown in Figure 5b).

Sequence	A. Control	B. Damp Heat with Bias 85 °C / 85 % RH		C. Thermal Cycling with load -40 °C / 85 °C		D. Alternating Seq. B/C	
	5 kWh·m ⁻² light soak						
Round 1		DH+	DH-	TC	TC	DH+	DH-
Round 2		DH+	DH-	TC	TC	TC	TC
Round 3		DH+	DH-	TC	TC	DH+	DH-
Round 4		DH+	DH-	TC	TC	TC	TC
Round n							

- DH refers to 1 000 h 85 °C / 85 % RH, IEC 61215-2 MQT 13.
- DH+(-) indicates +(-) voltage bias of 600 V or module's rated system voltage, whichever is greater, on the sorted module leads with respect to grounded frame.
- TC refers to 200 cycles between -40 °C and 85 °C, IEC 61215-2 MQT 11, but with I_{mp} applied when $T > 25$ °C during the ramp up in temperature.
- Alt. DH/TC refers to a sequence of alternating 1 000 h DH and TC 200 stress cycles described above.

IEC



b)

Most module types shown were run for five rounds. Rounds consisted of 200 thermal cycles or 1 000 h of damp heat with either + or - nameplate system-voltage applied. Module type 2 testing was terminated at three rounds of thermal cycles, and type 7, a latecomer to the program, was tested only through alternating DH (-) / thermal cycle for six rounds [12].

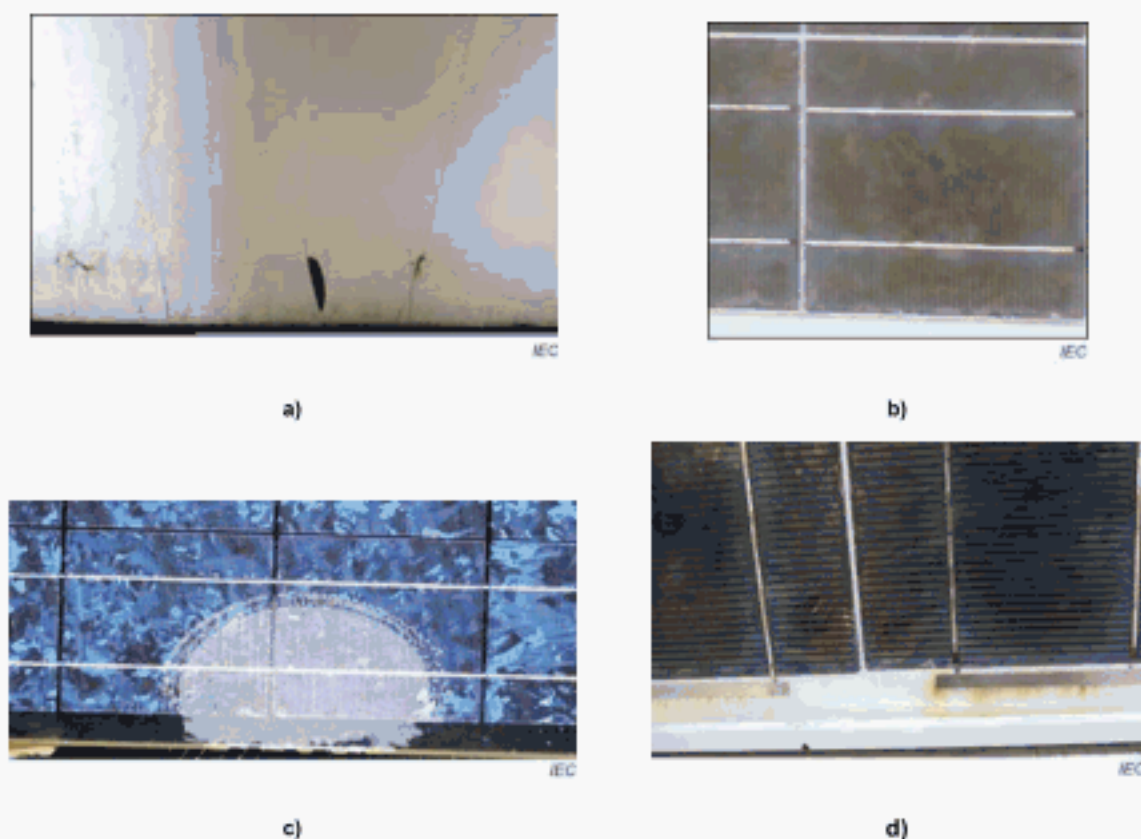
Figure 5 – a) Overview of the test-to-failure sequences, and b) results showing module power normalized to their post-light-soak values for seven module types

Module nameplate system-voltage (V_{sys}) bias of 600 V, either in (-) or (+) polarity, was applied to the active cell circuit in the DH environment, [DH (+), DH (-)]. These sequences discern susceptibility to various potential-induced degradation (PID) modes such as junction shunting, loss of surface passivation (polarization), and electrochemical reactions on the cell surface that may lead to delamination and loss of light transmission to the cell due to degradation of the antireflective coating or the encapsulant.

Modules tested through thermal cycling (TC) with the short-circuit current passing through the cell strings show mild degradation. In some cases, cracks propagated through cells that led to partially disconnected cell regions. In some cases, TC can lead to other issues including hot spots, interconnect fatigue, and solder-bond failure.

The alternating damp heat with bias and thermal cycling are sequences Alt DH (+ or -)/TC. DH may embrittle some polymers, and the thermal cycling applies some thermomechanical stress and causes desiccation that can lead to loss of toughness. Examples of degradation modes found when applying the TTF protocol are shown in Figure 6a) to d). Some of these degradation modes (backsheet cracking, delamination, and interconnect corrosion) have also been observed by others in their work on sequential and combined acceleration tests for crystalline silicon PV modules [13, 14]. The acceleration factors for these degradation modes are still being

studied. The levels of stress applied in the TTF are higher than in the natural environment, but the resulting degradation modes are frequently seen to be field-relevant considering their observation in the field [12]. These degradation modes were not seen in any of the single-factor tests such as DH, thermal cycling, or humidity-freeze tests. However, if modules are run for longer duration in single-factor tests, some of the degradation modes might eventually be observed. Because the levels applied in TTF exceed those of the natural environment, the mechanisms of degradation observed may be different, even if the modes appear the same. A summary of the sample type used, stress factors, and their sequence and combination, along with resulting degradation modes seen for the modules in the study, is given in Table 4.



- a) Backsheet embrittled in damp heat and cracked in the following thermal cycling;
- b) Degradation of silicon nitride antireflective coating in damp heat with positive system voltage bias applied to the cell circuit;
- c) Delamination of an ionomer-based thermoplastic encapsulant through 3 000 h damp heat and positive system voltage bias applied; and
- d) Corrosion, delamination, and ion migration around bus ribbon in 2 000 h of damp heat with positive system voltage applied [12].

Figure 6 – Examples of field-relevant degradation modes seen in modules tested in the test-to-failure protocol

Table 4 – Test-to-failure – Sequential test protocol

Sequential/ combined	Stress factor A	Stress factor B	Stress factor C	Combined stress effect(s)
	DH / F_{sys} bias (+) or (-)	TC with application of current	Cyclic application of stress factors A and B	
Material				
Coupon				
Mini-module				
Module	85 °C/85 % RH, +600 V or -600 V, 1 000 h	-40 °C/ 85 °C, <i>iso.</i> , 200 cycles	Stress Factors A and B	Backsheet cracking, corrosion, delamination, PID, solder-bond failure, antireflective coating degradation
Sequential/Combined: C = [A B] × n				

5.5 Sequential test protocol optimized for differentiating backsheets

Based on detailed field studies of module degradation modes, accelerated tests to better the failure mechanisms in backsheets have been devised after finding that single-factor stress tests capture some of the observed field failure modes, but that they miss others resulting from synergistic effects or combinations of stresses applied in a sequence. To address this, three sequential stress tests referred to as module accelerated stress tests (MASTs) were developed and applied; these are shown in Figure 7 [15] and summarized in Table 5 through Table 7. These were developed using mini modules, but some of these tests are also being extended to full size module.

The first of these tests, MAST #1, incorporated DH of 85 °C and 85 % RH in an initial exposure of 1 000 h. This duration is based on comparing the mechanical properties of backsheets from the field and backsheets exposed to the DH. Both modules exposed to this DH level and modules in the field for over a 25-year period using a polymer A-layered backsheet did not exhibit impaired mechanical properties, as confirmed by measurements of tensile strength and mechanical elongation to break tests. Exposure to greater than 1 000 h of DH was found to cause hydrolysis damage to the polyester core within the backsheet, leading to degradation in mechanical properties not seen in the field.

UV dose applied in the MAST assumes an albedo exposure of 12 %. The total UV exposure over 25 years of the back side of the PV module is estimated to be about 276 kWh/m² (300 nm to 400 nm) based on meteorological data in a desert climate. Four 1 000 h UV-A exposure segments at an intensity of 65 W/m² (300 nm to 400 nm) are employed in MAST #1. The test uses either a 70 °C black-panel temperature (BPT), with sample temperature of about 70 °C; or, for higher acceleration filtered Xe lamp exposure, 90 °C BPT with sample temperature of about 75 °C [16].

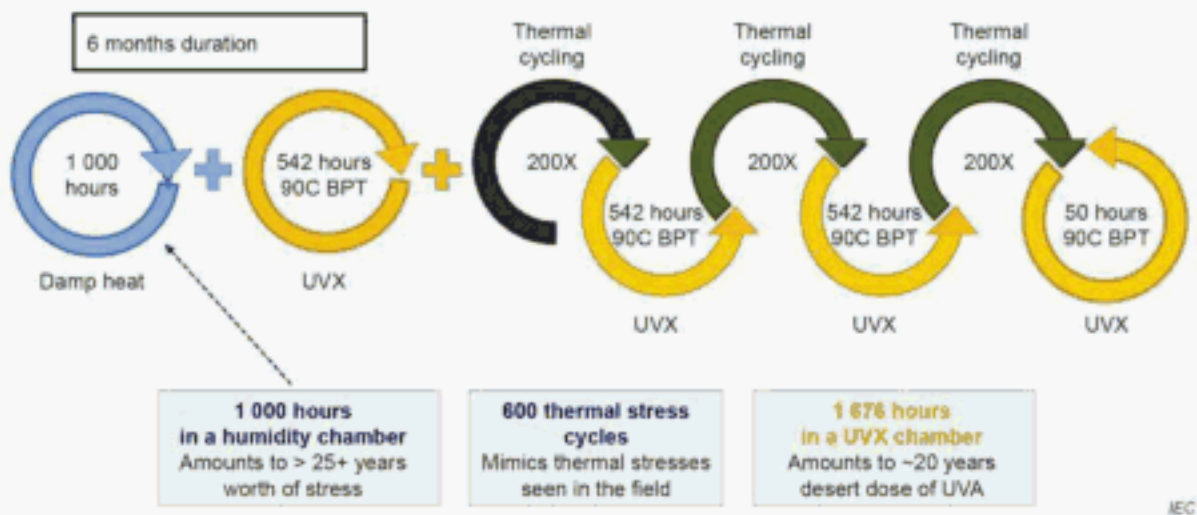
To apply thermomechanical stress, standard thermal cycling (-40 °C to 85 °C) up to 600 cycles is applied, which is commonly used in the industry for extended durability testing. Although not yet incorporated into a MAST, cyclic mechanical loading steps are also being studied for inclusion because they have been found to assist in replicating an encapsulant/glass interface delamination mode that has been observed in the field; this is discussed in 6.2.4. A summary of the sample type used, stress factors, and their sequence and combination, along with resulting degradation modes seen for the modules in the MAST #1 study, is given in Table 5.

Figure 8a) to d) shows optical photos of module degradation modes resulting from the MAST #1 testing, compared to images obtained from fielded PV modules. The images reveal cracks in a polymer B-based backsheet type after the second or third application of a UV-Xenon lamp

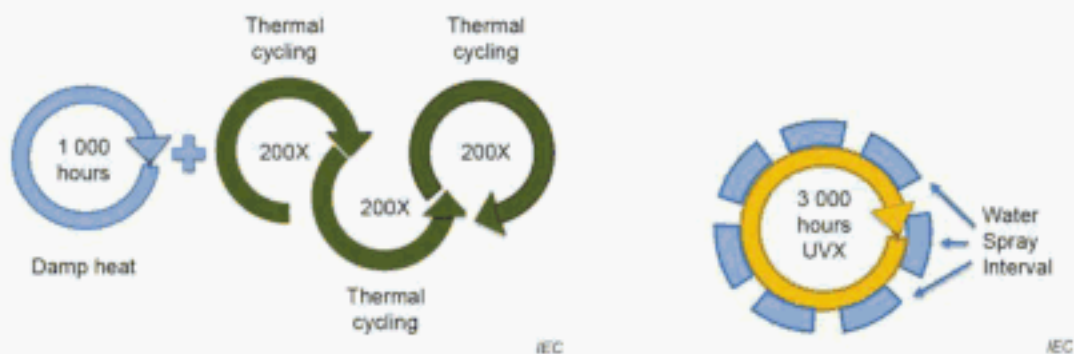
(UVX) sequence and in polymer C backsheets after the first application of the UVX sequence in MAST and also in the field.

In some cases, as in degradation of polymer C, the MAST #2 sequence without UV radiation could also result in backsheet cracking, indicating that UV radiation is not a critical factor for degradation of this material. Heat can be responsible for the cracking [17], and the cracks open initially over regions of high mechanical stress, including over tab ribbons and between cells in the module. A summary of the sample type used, stress factors, and their sequence and combination, along with resulting degradation modes seen for the modules in the MAST #2 study, is given in Table 6.

Yellowing of the inner layer occurring in a polymer B-based backsheet was shown with UV radiation in MAST #3 testing as in Figure 8(e). This type of construction also exhibited yellowing in the field as shown in Figure 8f) [18]. A summary of the sample type used, stress factors, and their sequence and combination, along with resulting degradation modes seen for the modules in the MAST #3 study, is given in Table 7.



a)



b)

c)

Figure 7 – Module accelerated sequential tests (MAST)

Table 5 – Module accelerated stress test 1 (MAST #1)

Sequential/ combined	Stress factor A	Stress factor B	Stress factor C	Combined stress effect(s)
	DH	UV	TC	
Material				
Coupon				
Mini-module	85 °C / 85 % 1 000 h	70 °C or 75 °C module temperature, 65 W/m ² (300 nm to 400 nm) 542 h	TC (-40 °C/ 85 °C)	Backsheet cracking
Module				
Sequential: A B [C B] × n				

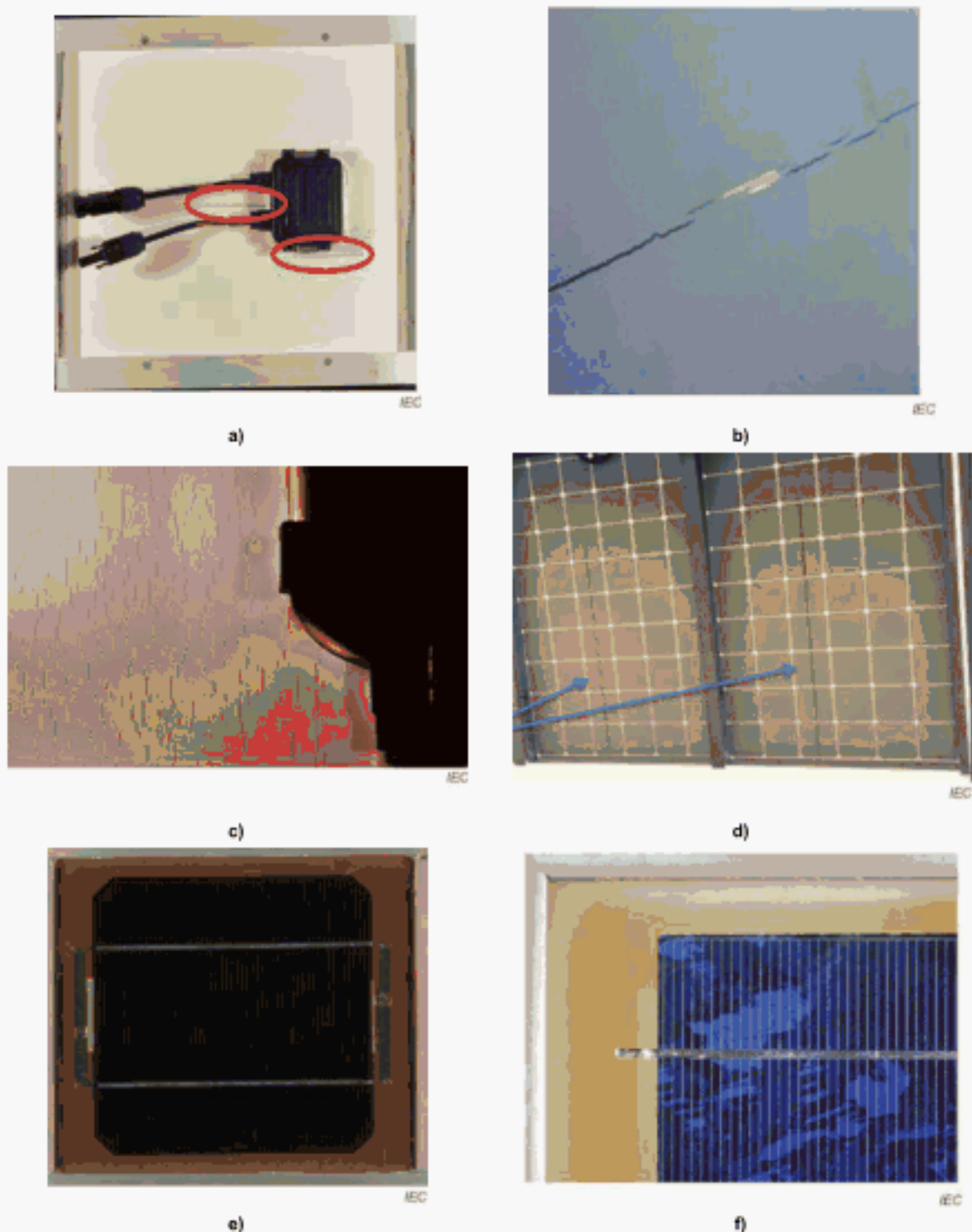
Table 6 – Module accelerated stress test 2 (MAST #2)

Sequential/ combined	Stress factor A	Stress factor B	Combined stress effect(s)
	DH	TC	
Material			
Coupon			
Mini-module	85 °C / 85 % RH 1 000 h	3 x TC 200 (-40 °C/ 85 °C)	Backsheet cracking (polymer C)
Module			
Sequential: A B			

Table 7 – Module accelerated stress test 3 (MAST #3)

Sequential/ combined	Stress factor A	Stress factor B	Combined stress effect(s)
	UV + T	Water spray	
Material			
Coupon			
Mini-module	90 °C, 123 W/m ² (300 nm to 400 nm) 102 min	18 min (with UV component of Stress Factor A)	Backsheet yellowing Backsheet cracking
Module			
Sequential: A B × 1 500 cycles			

Sequences using the various capability of weathering chambers were also explored, including intermittent light and water-spray cycling. Initial efforts were based on a standard weathering sequence (ASTM G155) incorporating such water spray, which provides both an added moisture component and mechanical stress from thermal shock. Inner-layer cracking of PET-based backsheets was produced on a mini-module as shown in Figure 9a) after exposure from the front with filtered Xe light and front-side water spray (3 500 total hours of filtered exposure, 123 W/m², 300 nm to 400 nm, 90 °C BPT; 102 min UV radiation under dry conditions and 18 min in the dark with water spray cyclically applied). Similar inner-layer backsheet cracking in fielded modules is also seen in Figure 9b), where the cracks do not extend behind the cells, which indicates a photolytic degradation mechanism. Further information about the degradation and failures studied in this clause can be found in in references [19, 20].



- a) Polymer C-based backsheet tested through MAST #1 displaying cracking, also reproducible without UV with MAST #2;
- b) Polymer C after five years in the field also showing cracks;
- c) Polymer B backsheet through MAST #1;
- d) Polymer B after five years in the field (arrows point out cracked and peeling areas);
- e) Front-side UV exposure and 90 °C black-panel temperature through MAST #3 for a mini-module with a polymer B backsheet type showing significant discoloration; and
- f) Front-side yellowing in the field for the polymer B backsheet occurring in five years [15, 20].

Figure 8 – Degradation modes from MAST and fielded modules

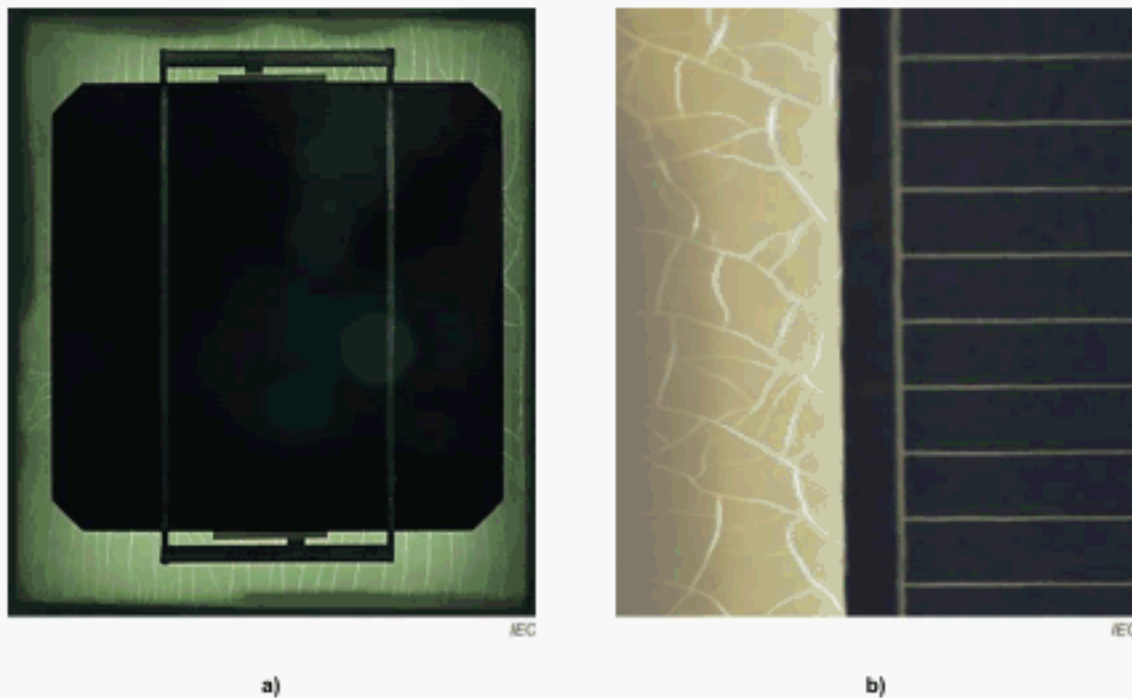


Figure 9 – a) Front-side mini-module exposure in a xenon weathering chamber with water spray; b) fielded module with six years of service in North America with 30 % power loss [21]

5.6 Mechanical stress testing in combination with damp-heat, humidity-freeze, and thermal-cycling tests for examining cell cracking and its effects

Snow loading and wind loading events lead to deflection in the module, which causes various degradation modes such as crack growth in cells. For example, the change in module power through a windstorm with gusts of 16 m/s was studied. The storm resulted in maximum (peak-to-peak) displacement of 1,6 cm. The maximum displacement in the positive direction (up) was about 0,9 cm and about $-0,77$ cm in the negative direction (down). The event led to a loss in maximum power of 2,4 % (relative) attributed to expansion of existing cracks rather than the creation of new cracks [22]. Therefore, crack prevention before or during installation was concluded to be critical for mitigating power loss by crack propagation in the field.

After the introduction of cracks, which may not result in significant power loss, thermal cycling and humidity-freeze stress tests will drive crack growth, and the module will likely show additional loss in power. An example is shown in Figure 10, where a modified IEC 61215-2 static mechanical load (SML) test was applied (2 400 Pa applied two times per side), followed by thermal cycling and humidity-freeze testing, and further stages of mechanical loading and chamber testing [23]. At stages III and stage VI, after the mechanical-loading stages, thermomechanical stress is introduced by thermal cycling and humidity freeze, where a greater drop in the cell performance parameters is often observed. A summary of the sample type used, stress factors, and their sequence and combination, along with resulting degradation modes seen for the modules in the study, is given in Table 8.

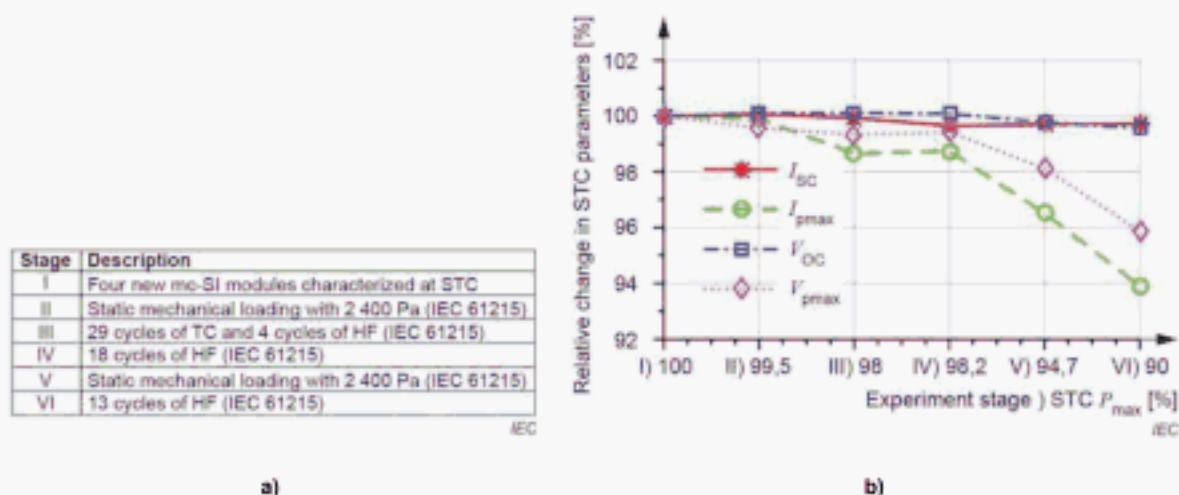


Figure 10 – a) Test-stage description; b) relative change in standard test condition (STC) module parameters as a function of stage and maximum power determined at STC [23]

It has also been shown that after loading a module with a static load, or after walking on a module, the power is not necessarily changed. However, while applying a load (as in a strong wind load), the module deflects and existing cracks in the cell expand in width, leading to power loss from electrically isolated cell parts [24].

Evaluation of test sequences to examine vulnerabilities with respect to mechanical stress is ongoing. For example, studies show that a single exposure to low temperature introduces fracture of silicon solar cells [25]. The mechanism proposed is the contracting encapsulant bending the cell near the interconnect ribbon, which results in high tensile stress on the back of the cell. An alternative explanation is concentration of thermally-induced stress in the Si from contracting interconnect ribbon. Low temperature results in crack formation, where cracks can expand under subsequently applied stress. The frequency used during cyclic dynamic mechanical load (DML), as outlined in IEC TS 62782, also affects power loss. After 50 thermal cycles, 10 humidity-freeze cycles, and static-load testing are performed, the application of the same number of cycles at a greater frequency (at the same applied load) yielded a lesser power loss [22].

Table 8 – SML-TC-HF sequential test

Sequential/ combined	Stress factor A	Stress factor B	Stress factor C	Combined stress effect(s)
	SML	TC	HF	
Material				
Coupon				
Mini-module				
Module	2 400 Pa (IEC 61215-2, modified)	TC (IEC 61215-2, modified)	HF (IEC 61215-2, modified)	A greater drop in the performance parameters after TC and HF test; cell cracking
Sequential: A B C A C				

6 Mechanism-specific multi-factor stress tests

6.1 General

This clause discusses how stresses applied in chamber tests in combinations as they appear in the natural environment lead to the revelation of field-relevant degradation modes in PV modules that single-factor tests do not appear to show.

6.2 Testing for delamination

6.2.1 General

Delamination is one of the most-frequently observed PV module degradation modes. By one estimate, it is the second-most-cited issue [26]. A number of different kinds of delamination are observed in the field, such as delamination at the encapsulant, front glass, cells, interconnect ribbons, and backsheet interfaces. These have different mechanisms that are enabled by differing stress factors. Delamination may further facilitate subsequent module degradation such as corrosion due to increased moisture ingress. We next review a subset of the delamination mechanisms observed in the field and show how a combination of stresses is involved in their manifestation.

6.2.2 Delamination – UV irradiation with high-temperature stress

A study of the delamination occurring between the EVA layer and the antireflective coating on the cell in fielded crystalline silicon modules was performed [27]. Cell surfaces were coated with TiO₂ and SiO₂ antireflection films. Raman spectroscopy showed that the crystal structure of TiO₂ used in the antireflective coating was of the anatase type. TiO₂ in the anatase phase is a photocatalyst for many reactions. Therefore, it may inadvertently promote oxidation or other reactions at the interface between polymers and the cell under UV radiation, believed in part to be responsible for delamination seen in the study. Delamination of this type is sometimes seen in more cells in front of the junction boxes, where the module temperature is hotter in operation.

It was also reported that the delamination of some encapsulants within a PV module could be induced by UV irradiation with high intensity at a high temperature [28]. In a commercially available PV module type with a conventional architecture (front glass–EVA–cell–EVA–backsheet), delamination occurred around the busbars on a PV cell by the irradiation of UV radiation (180 W/m² in the range of 300 nm to 400 nm) at 65 °C for 100 h, and the area of delamination expanded with increasing duration of exposure to these combined stresses as in Figure 11a). In contrast, no delamination was detected when a replica of this PV module type was exposed in the dark condition at 75 °C for 1 000 h; Figure 11b). However, a minimal amount of delamination resulting from exposure at 90 °C without UV irradiation was noted in this study [28]. The precise mechanism(s) on the combined effects of UV radiation and heat in this study have not been clarified; but it is possible that photocatalytic reactions involving the materials used, such as silver of the grid fingers in the modules, may have promoted the delamination. A summary of the sample type used, stress factors, and their sequence and combination, along with resulting degradation modes seen for the modules in the study, is given in Table 9.

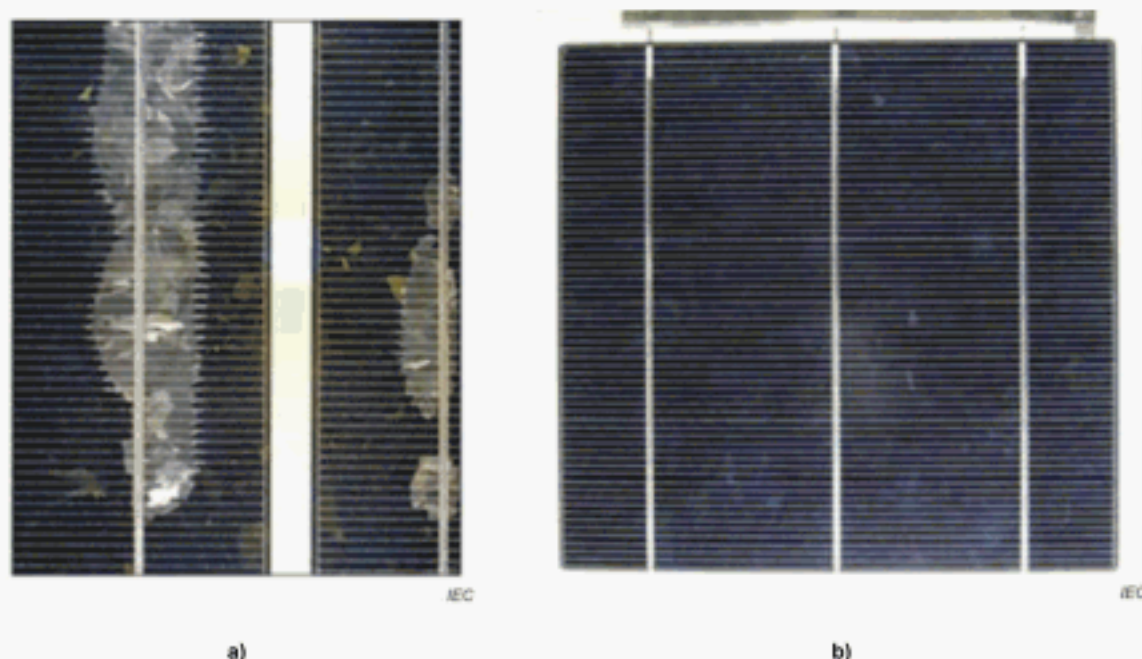


Figure 11 – a) Stress testing at 65 °C combined with UV radiation dose of 180 W/m² in the range of 300 nm to 400 nm, 900 h; b) 75 °C without UV radiation, 1 000 h [28]

Table 9 – UV irradiation under high-temperature conditions

Sequential/	Stress factor A	Combined stress effect(s)
	UV + T	
Material		
Coupon		
Mini-module		
Module	180 W/m ² at 65 °C, 100 h	Delamination
Stress factor A: UV radiation with elevated temperature.		

6.2.3 Delamination – UV irradiation with thermal-cycling stress and humidity freeze

In addition to the observation of delamination in 6.2.2 above associated with the factors of UV radiation and heat, a combined effect of UV irradiation with thermal cycling stress was observed [27]. When the PV module was exposed to a thermomechanical stress induced by cycling the module temperature between –20 °C and 75 °C with 1 h dwells at each extreme, slight delamination was observed at the EVA/cell interface along the busbars within 75 cycles of the thermal cycling with UV irradiation of 180 W/m² in the range of 300 nm to 400 nm applied only during the high-temperature dwell. This contrasts with modules that did not exhibit delamination after 75 cycles of thermal-cycling testing without UV irradiation (i.e., continuous dark condition). A summary of the sample type used, stress factors, and their sequence and combination, along with resulting degradation modes seen for the modules in the study, is given in Table 10.

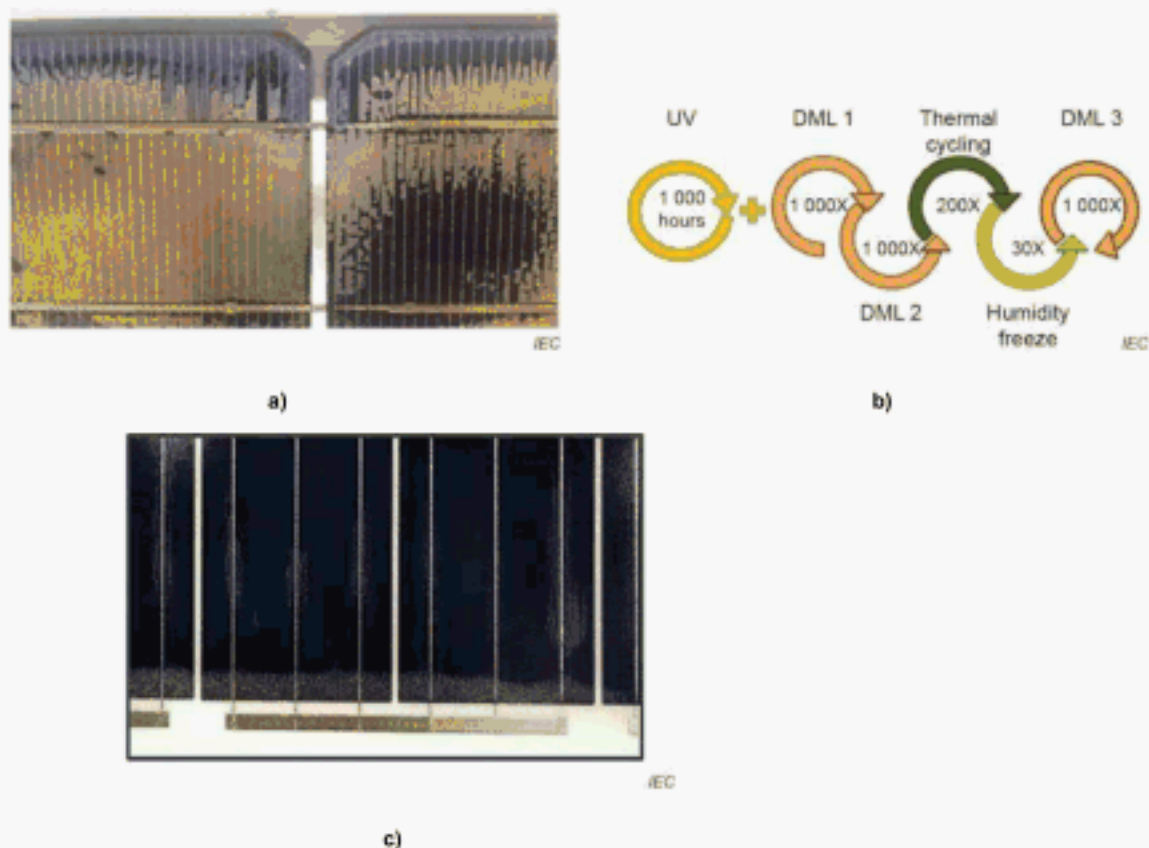
Table 10 – UV irradiation with TC stress

Sequential/ combined	Stress factor A	Stress factor B	Combined stress effect(s)
	UV + T	TC	
Material			
Coupon			
Mini-module			
Module	180 W/m ² at 75 °C module temperature, 1 h	-20 °C / +75 °C, 1 h dwells	Delamination starting after 75 cycles, significant at 125 cycles
Combined: A + B			

6.2.4 Delamination – UV irradiation with cyclic dynamic mechanical loading, thermal cycling stress, and humidity freeze

A study compared some crystalline-silicon glass-backsheet film (GB) modules with crystalline-silicon glass-glass (GG) modules, which have shown a prevalence of delamination as illustrated in Figure 12a) [21]. Commercial GB and GG modules were tested with EVA encapsulant and 2,5 mm thick glass on both sides of the GG module and 3,2 mm glass in the GB module. Delamination observed in the GG module is sometimes associated with the low permeability of the glass-glass structure such that any expanding reaction products trapped within the GG laminate cause bubble formation, initiating the delamination. Other factors affecting the stress state in the modules, such as whether rigidity of the glass can impede compliance to thermomechanical stress, are being explored [18].

To test for the module's capability to perform in a dynamic environment with a combination of stresses including wind loads that may be triggering delamination, tests were developed consisting of frontside UV-A (340 nm peak) light exposure, a cyclic DML sequence, 200 thermal cycles, and 30 cycles of humidity-freeze testing (IEC 61215-2-type) as shown in Figure 12b). DML 1 consists of 1 000 cycles of $\pm 1\,500$ Pa of loading at 0,167 Hz and DML 2 consists of 1 000 cycles of $\pm 1\,500$ Pa of loading at 1 Hz at room temperature. The GG construction showed delamination along the edges and tabbing ribbon, developing and expanding inward over the cells during the course of this test sequence as seen in Figure 12c), shown after the humidity-freeze step. The final proposed stage, DML 3, was not performed because the samples had already exhibited delamination. The glass-backsheet-type module run in parallel only exhibited minor yellowing. A summary of the sample type used, stress factors, and their sequence and combination, along with resulting degradation modes seen for the modules in the study, is given in Table 11.



- a) An example of delamination from a fielded glass-glass module after 21 years; b) A sequential test to replicate the environment with UV radiation, cyclic dynamic mechanical loading, thermal cycling, and humidity freeze; and c) Delamination of a glass-glass module after the humidity-freeze part of the test sequence shown in b) [21].

Figure 12 – Delamination in sequential test

Table 11 – UV irradiation with DML-TC-HF sequential test

Sequential/ combined	Stress factor A	Stress factor B	Stress factor C	Stress factor D	Combined stress effect(s)
	UV	DML	TC	HF	
Material					
Coupon					
Mini-module	UV A (65 W/m ²) 70 °C) 1 000 h	±1 500 Pa, 0,167 Hz, room temperature 2 x 1 000 cycles	IEC 61215-2 200 cycles	IEC 61215-2 30 cycles	Delamination in a glass-glass module
Module					
Sequential: A B C D B					

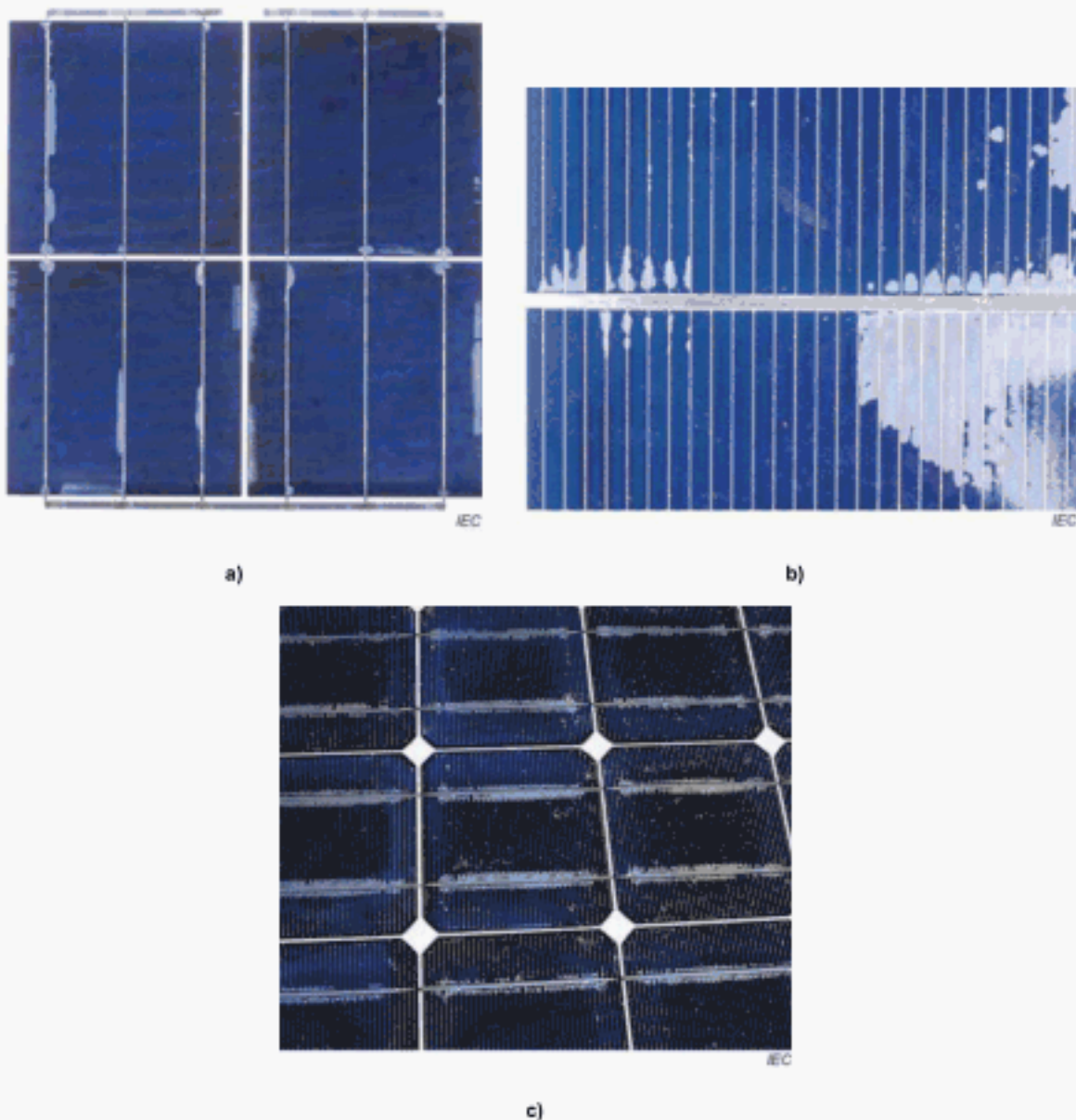
6.2.5 Delamination – Temperature, humidity, and electric field associated with system voltage

Researchers [27] measured Na accumulation at the delaminated interface in fielded modules. Sodium at the cell surface has been associated with reduced adhesion in PV modules [29]. It has been shown that V_{sys} stress [26, 30] with the cells in negative bias leads to the migration of Na⁺ ions to the cell surface [31]; as a result, a reduction of adhesion can be seen, especially

at the Ag metallization where it collects [31, 32]. Humidity is also a factor leading to reduced

adhesion of Ag to the encapsulant; but the adhesion is reduced faster when there is negative V_{sys} bias (i.e., $-1\,000\text{ V}$) on the cells [33]. In addition, electrical potential can drive cathodic reactions, leading to effluence of hydrogen gas that can cause delamination [32, 34]. The V_{sys} bias, and as a result, the nature of the ionic current that flows through the module, affects the pH in the encapsulant and consequently the type of chemical reactions that can occur [32]. Therefore, in most any module durability test, especially those concerning corrosion, it is critical to include the factor of V_{sys} stress to represent the behaviour in the natural environment.

Mini-modules subjected to DH at 85 °C and 85 \% RH for $1\,000\text{ h}$ were left to dry for an extended period of time before being subjected to a PID stress at 72 °C and 95 \% RH , with a negative bias of $1\,000\text{ V}$ with the modules' face grounded using Al foil. As seen in Figure 13a) and b), areas of delamination appeared that are similar to those seen in PV modules fielded for 20 years shown in Figure 13c). This test was repeated on several mini-modules of a given construction, varying the PID stress-test exposure time. After a PID stress on the order of 110 h , only a very small amount of delamination was visible. After an additional 137 h of continued stress, the delamination area significantly increased [26]. Summarization of the sample type used, stress factors, and their sequence and combination, along with resulting degradation modes seen for the modules in the study, is given in Table 12. With this method, evaluation of module laminates for the PID-delamination mode was incorporated into IEC 62804-1-1.



a) and b) show examples of delamination between EVA encapsulant and cell after exposure to 85 °C and 85 % RH damp heat and then subjected to a PID test at 72 °C and 95 % RH with a negative bias of 1 000 V, imaged here after 196 h.

c) A fielded PV module in Florida shows similar delamination in the vicinity of the tab ribbons and at cell edges [26].

Figure 13 – Delamination associated with system voltage

In 60-cell commercial crystalline silicon modules tested in the same way, all modules with leakage current density of $4,9 \text{ nA}\cdot\text{cm}^{-2}$ or below measured during the application of the 72 °C and 95 % RH, with $-1\,000 \text{ V } V_{\text{sys}}$ showed no delamination between the cell and the EVA. Another module with a higher leakage current of $16 \text{ nA}\cdot\text{cm}^{-2}$ exhibited severe delamination over the course of the test, clearly observable at 156 h of stress [30].

Table 12 – DH – Negative system bias stress sequential test

Sequential/ combined	Stress factor A	Stress factor B	Combined stress effect(s)
	DH	DH and V_{sys} bias (-)	
Material			
Coupon			
Mini-module	85 °C / 85 % RH 1 000 h	72 °C / 95 % RH / –1 000 V	Delamination: Stress factor B 110 h, small; 247 h, significant
Module	85 °C / 85 % RH 1 000 h	72 °C / 95 % RH / –1 000 V	Significant delamination: Stress factor B 156 h
Sequential A B			

6.3 Testing for potential-induced degradation

6.3.1 General

System voltage can produce power loss by PID, for example, by shunting (PID-s) and polarization (PID-p). The following subclauses examine how some of the other stress factors of the natural environment affect PID rate.

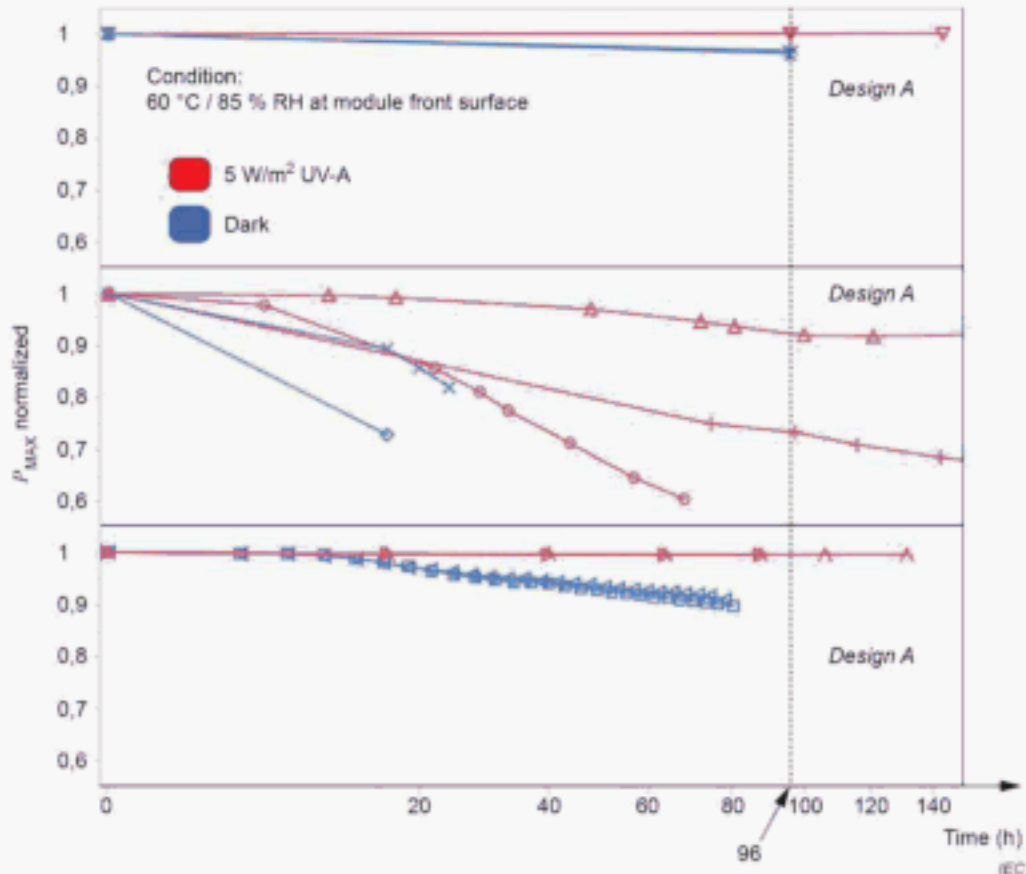
6.3.2 Testing for potential-induced degradation with humidity, voltage, bias, and light

Modules are known to degrade by PID-s under the factors of temperature, which drives increased ionic conduction; humidity, providing surface conduction and also an extent of increased conduction if it penetrates the module; and voltage bias (negative bias to cell), which forms the electric field that causes drift of Na^+ ions toward the cell, causing shunting of the cell junction [35]. Effects of illumination simultaneous to applying voltage bias have been studied for polarization, which is the accumulation of charge in the passivation and antireflective layers leading to increased surface recombination and lower cell voltage. It was reported that UV radiation will ionize carriers in the silicon nitride antireflective coating leading to photoconductivity, and enabling charge conduction and reducing the electrical potential across the nitride [36]. Further, any photoionized electrons in the antireflective coating or its interfaces may neutralize advancing positive charge.

To quantify the effects of the light in the UV region, which has the potential to change the degradation rate of modules under V_{sys} bias, three module designs were stress tested for PID in the chamber with and without 5 W/m² of UV-A band illumination [37]. Glass surfaces were maintained at (60 ± 1) °C, and (85 ± 3) % RH providing humidity to maintain the surface conduction via adsorbed water.

The results shown in Figure 14 for the dark-chamber PID tests performed according to IEC TS 62804-1 stress method a) at the 60 °C level show that module types A and C exhibit better PID resistance than type B. The degradation in types A and C is eliminated when placed under illumination along with PID stress of 1 000 V within the timeframe examined—about 96 h. The polarity of the voltage bias applied was consistent with the module's PID-sensitive polarity. Type B degraded faster in the dark relative to the other designs, and the degradation was not entirely eliminated by the 5 W/m² UV-A illumination with a fluorescent lamp centred at 340 nm, but it was slowed [37]. Reference [36] discusses how UV radiation photoconductivity causes shunting over the thickness of the antireflective coating and provides a recovery effect, which must exceed the rate of degradation in the dark to arrest polarization. Further examples of light affecting degradation rate by polarization-type PID mechanisms in various cell types can be found in [38]. It has also been reported that the state of bias in the junction (such as open-circuit, short-circuit, or maximum power) affects the PID rate in the shunting mode (PID-s) [39]. In view of these sensitivities, it would be most meaningful to test for PID under light with the module connected to a load as it would be in a PV system; however, the situation of partial

shading (e.g. fallen and adhered foliage) may also occur, so characterization for shadowed areas is also required. A summary of the sample type used, stress factors, and their sequence and combination, along with resulting degradation modes seen for the modules in the study, is given in Table 13.



The 5 W/m² UV-A irradiance on the module superstrate slows or arrests the degradation [37].

Figure 14 – Degradation of three modules with and without UV-A light irradiance in chamber at 60 °C, 85 % RH, and 1 000 V (positive or negative polarity depending on the sample)

Table 13 – UV irradiation – negative system bias stress combined test

Sequential/ combined	Stress factor A	Stress factor B	Combined stress effect(s)
	DH	DH / V _{sys} bias (-)	
Material			
Coupon			
Mini-module			
Module	UV-A: 5 W/m ²	60 °C / 85 % RH (module surface) / -1 000 V, 96 h	Elimination or slowing of PID-shunting and polarization
Combined: A + B			

6.3.3 Factor of salt mist

For space-constrained areas, reducing evaporation, and to use existing electrical grid infrastructure, there is increasing interest in PV installations floating on water. Both freshwater

and saltwater installations have been implemented. Floating installations bring the concern about how the combination of increased humidity, sea salt, and even bird droppings will affect a number of degradation modes, including PID [40, 41]. Sea salt deposited on glass module surfaces yielded up to a 3,5 order-of-magnitude decrease in resistance on the glass surface when the RH increased over the RH range of 39 % to 95 %, compared to an unsoiled control that displayed less than one order-of-magnitude increase as seen in Figure 15 [41].

The transport of sodium ions into a PV module (through the backsheet) has also been suggested [40], although the precise mechanism(s) that would enable such transport of sodium ions has not been clarified. A combined or sequential test involving salt mist is anticipated to be beneficial to characterize the degradation of module installations in coastal regions.

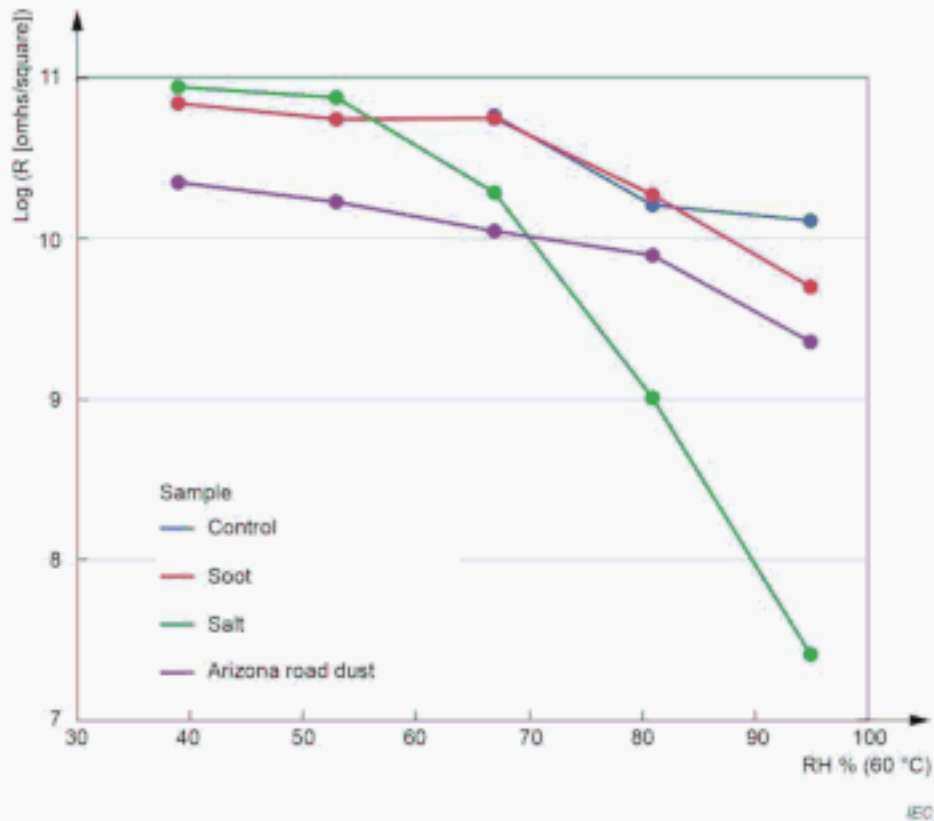


Figure 15 – Sheet resistance measured on glass surfaces with various soil types, as a function of relative humidity (RH %), at 60 °C [41]

6.4 Testing in damp heat with current injection and as a function of temperature

Injection of current (or forward biasing the solar cells) during aging achieves three conditions: First, it places the junctions of the cells in a more field-representative state—the offset of the n and p regions of the solar cells approaches the state under illumination with a connected load, which is reduced from that of the open-circuit condition. As a result, any mobile ions in the absorber may drift because of the electric field or may diffuse in a manner more closely resembling the transport in fielded modules. Second, it creates a supply of carriers, as exists during daylight, which can populate carrier traps or states in the semiconductor absorber. Third, it leads to Joule heating when current flows through resistive materials or at restrictive locations (e.g., solder joints). On the other hand, forward biasing the cells in the dark leads to current flow in the opposite direction as under light because dark forward bias is first-quadrant operation in the diode curve, whereas under light, the diode is operating in the fourth quadrant. The effects of irradiance also differ from electrical injection because electrical injection of current does not produce short-wavelength ionizing radiation that the sun or a full-spectrum solar simulator produces, which can affect and degrade layers of the solar cell and module encapsulation. Therefore, dark current injection can only activate a subset of degradation

modes. A most comprehensive analysis of the degradation modes in a module will therefore require using a broadband light source.

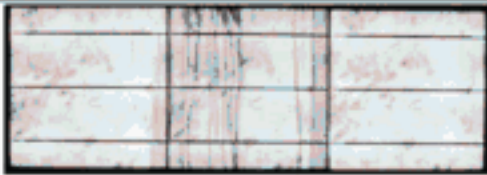
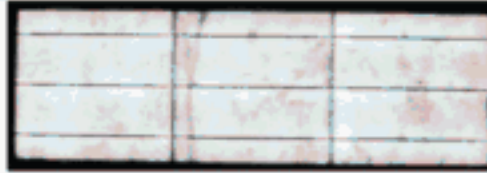
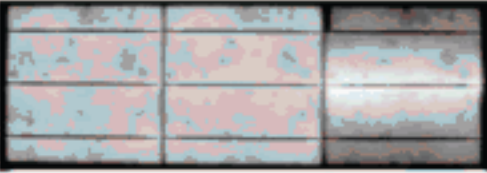
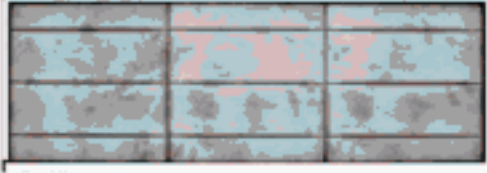
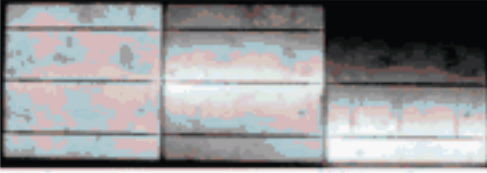
The temperature used during accelerated testing can activate different degradation mechanisms in the cell. For example, applying voltage potential over the module terminals for the injection of dark forward-bias current, as with illumination, can produce light-induced degradation (LID) [42] and light- and elevated-temperature-induced degradation (LeTID) [43, 44]. However, testing at a single temperature will not give a complete story. During stress testing under light at high temperature (e.g., 85 °C), LID associated with the boron-oxygen complex will be driven toward a stabilized state [45] and this LID mechanism may not be seen. The LeTID mechanism (believed associated with hydrogen migration and its binding to a defect leading to carrier recombination [46]) may be seen at 85 °C, leading to a decrease in sample performance, often followed by a slow rise in module power [43]. Considering this example of how the different mechanisms manifest at different temperatures, it can be seen that single, constant temperature accelerated stress tests appear insufficient for evaluation of PV modules.

Additionally applying short-circuit current into the PV module during a conventional (IEC 61215-2) DH stress test has recently demonstrated that degradation of power by FF loss was accelerated by a factor of 1,42; this result follows from an increase in module temperature of 5 °C in the DH test condition [47]. DH with current bias may also accelerate degradation modes observed in DH with no electrical bias including ribbon corrosion, finger corrosion, and EVA discoloration [47]. It may additionally cause changes in LID, LeTID and PID states. Equilibrium humidity on the module during DH (with bias) would be somewhat lower due to Joule heating, but there would still be concerns about the degradation modes associated with the elevated humidity diffused into the module and externally applied electrical power because the DH humidity levels applied far exceed that of fielded modules.

Based on these results, incorporating current injection during accelerated testing may be considered for reproducing degradation modes including corrosion, delamination, and other degradation modes associated with current injection and to quantify the resulting power loss. However, electrical bias will not produce all the potential degradation mechanisms to which the module may be susceptible as with the application of UV-containing solar-spectrum illumination that produces photogenerated charge carriers, photochemical reactions, and additional degradation mechanisms. Further, light irradiation on the module when in combination with DH heats it, leading to more realistic levels of contained humidity.

6.5 Cell cracking and propagation in cyclic loading at various temperatures

Cell cracks and ribbon fractures induced by thermomechanical stress have been suggested to be affected by the mechanical properties of the encapsulant used in crystalline-silicon PV modules. The Young's modulus of EVA increases by around two orders of magnitude between ambient and –40 °C, making the encapsulation material much stiffer at lower temperatures. This large change in mechanical stiffness as the temperature is reduced has been reported to adversely affect the integrity of solar cells encapsulated in EVA, leading to both an increase in the number of cracks and increased crack length in encapsulated silicon cells when static or cyclic loads are applied [48].

Temp.	Press from Front Glass Side	Press from Backsheet Side
-20 °C	 20 000 cycles Cell cracks (hard)	 20 000 cycles Cell cracks (hard)
25 °C	 20 000 cycles Cell cracks	 30 000 cycles Ribbon fracture
80 °C	 10 000 cycles	 10 000 cycles Ribbon fracture

IEC

Figure 16 – Cyclic unidirectional 4-point bending with loading alternating between 0 N and 500 N at different temperatures, with duration of 4 s at each of the high- and low-pressure dwells, 10 000 to 30 000 cycles with pressure (“Press”) from the front-glass side or backsheet side [49]

A published report on the failure modes under differing temperatures and bending directions provides some information on how to more comprehensively represent mechanical stresses in accelerated testing [49]. This report found that initiation and propagation of cell cracks was induced at low temperatures. Ribbon fractures, which were induced only by the cyclic force from four-point bending from the backsheet side, were accelerated by higher temperature; see Figure 16. These tests help in evaluating the durability of ribbons, and factors such as cell alignment (e.g. distance between adjacent cells), cell thickness, ribbon dimensions, non-soldering distance from the cell edge, and bends or kinks in the ribbons that interconnect cells. However, the stresses within the samples in this study were not representative of the those experienced by PV modules (the stresses depend on the module geometry and boundary conditions constrained by factors such as the module frame and mounting). Thus, the durability or susceptibility to these stresses should ultimately be determined using the PV module as opposed to coupon and mini-module samples. Summarization of the sample type used, stress factors, and their sequence and combination, along with resulting degradation modes seen for the modules in the study, are given in Table 14.

Table 14 – Bending load test at various temperatures

Sequential/ combined	Stress factor A	Stress factor B	Combined stress effect(s)
	Bending load	Temperature	
Material			
Coupon			
Mini-module	500 N, ~30 K cycles	-20 °C, +25 °C, and +80 °C	Low temperature: Cell cracking; High temperature: Ribbon fracture
Module			
Combined: A + B			

7 Combined accelerated stress testing

7.1 Combined accelerated stress testing for tropical environments

Sequential tests of PV modules often involve moving samples through a series of single- or multi-factor tests found in IEC 61215-2. In contrast, combined-accelerated stress testing (C-AST) involves applying stressors in combinations that are seen in the natural environment. An example of a testing protocol developed with this philosophy is ASTM D7869 for paint and coatings used in the automotive and aerospace industries [50]. This test sequence cyclically applies periods of DH with water spray in darkness followed by periods of irradiance and higher temperature with lower humidity levels. This testing protocol has been extended in C-AST for testing of PV modules.

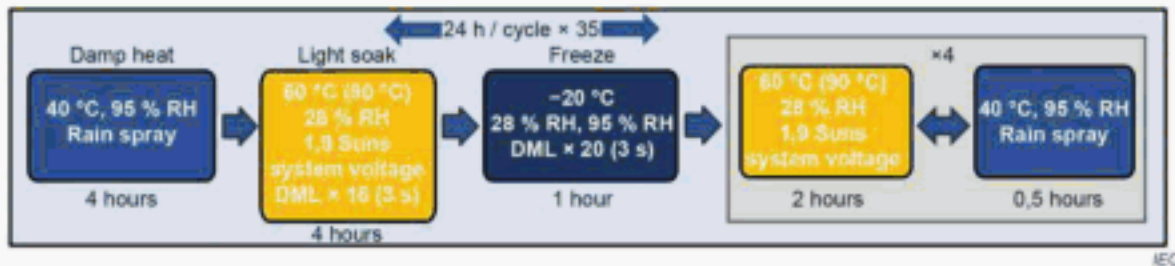
The ASTM D7869 standard was designed as an accelerated test for the environment of Miami, Florida (USA). It maintains realistic levels of stress for hot humid environments [51]. For example, the upper chamber air level for DH in ASTM D7869 under light (when the sample under test is hottest), 50 °C, 50 % RH [50, 51]. For example, the chamber air in ASTM D7869 under light (when the sample under test is hottest), 50 °C and 50 % RH [50], closely resembles the maximum humidity levels seen in tropical environments according to the IEC standard for classification of environmental conditions IEC 60721-2-1, 35 g/m³ the diurnal cycle occurring in the natural environment, high humidity with water spray and the filtered Xe-arc full-spectrum light are not applied together in [52]. High temperature represents according to ASTM D7869. The acceleration of the ASTM D7869 test over the south Florida environment was measured to be in the range of 8 to 16 [51].

A weathering chamber was customized for application of ASTM D7869. It was modified for the additional requirements of PV modules [53] resulting in the cyclically applied 24 h sequence shown in Figure 17. The modifications are as follows:

- Increasing the chamber air temperature for the upper temperature and irradiance dwells from 50 °C to about 60 °C to achieve the higher levels of the upper statistical tail of operating temperature that roof-mounted modules applied directly into an insulating surface can experience, 90 °C [54]. To counterbalance the increased chemical activity of the water at this higher temperature, the humidity level at the high-temperature stages was reduced to about 28 % to maintain the dew point at about the same level as in ASTM D7869 and near that of the maximum humidity level seen in IEC 60721-2-1 for tropical climates, 35 g/m³
- A freeze was included in each 24 h cycle, considering that the Florida environment exhibits freezes and that modules must be capable of resisting damage from freeze.
- PV modules were connected to a variable resistor for electrically loading them to their maximum power point and to a high-voltage source simulating system voltage with leakage current monitoring on the high-voltage supply side.

- d) Mechanical stress was applied with polytetrafluoroethylene-covered donut-shaped actuators that press down on the module surface to simulate a wind or snow load. The radius of curvature during application of pressure is set to match that of a full-size module when loaded at IEC 61215-2 static mechanical load (SML) level (2 400 Pa) or IEC TS 62782 DML level of 1 000 Pa. The equipment in this work only applies pressure on the lamp-facing side, at 0,125 Hz frequency (adjustable). The downward displacement occurs in about 0,1 s, followed by a slower release.
- e) Filtered Xe-arc lamps producing UV radiation with high fidelity to the solar spectrum (ASTM D7869 compliant filters) are applied to the normally light-facing side of the modules, and aluminium reflector troughs are mounted under the modules to achieve about 10 % of the front-side illumination in albedo on the rear measured at 340 nm.

The first experiment through C-AST involved a materials study using passivated emitter and rear cells (PERC), two encapsulants (UV-pass and UV-block) and three backsheets (polymers A, B and C) that were laminated in four-cell mini-modules [55]. The degradation modes that could be observed in some of the modules through application of the C-AST protocol shown in Figure 17 are given in Table 15, along with the mechanisms attributed and stress factors chiefly responsible.



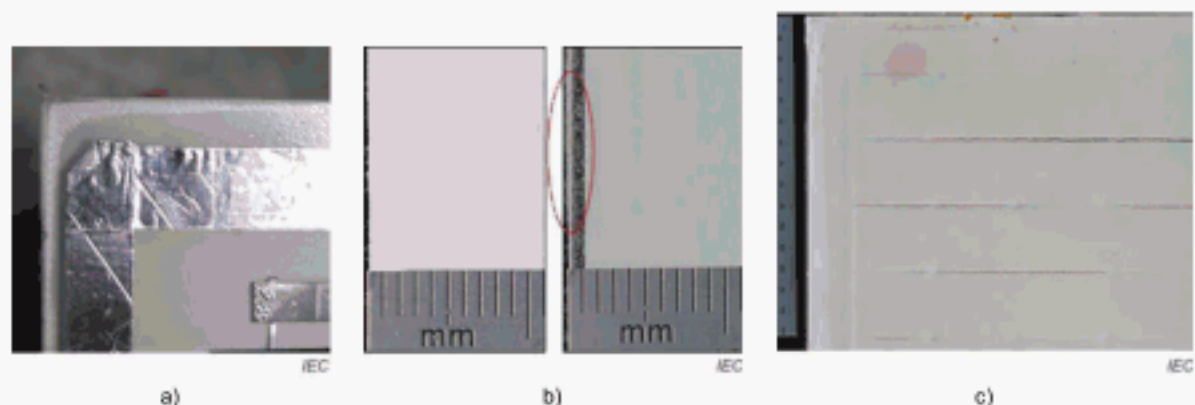
Times shown do not include ramps of temperature humidity and light. Module temperature, when different from chamber air temperature, is shown in parentheses.

Figure 17 – Example of 24 h PV module combined accelerated stress-testing protocol modified from ASTM D7869

Table 15 – Partial list of observed degradation modes, attributed mechanisms, and stress factors seen in the first application of the combined accelerated stress-testing protocol based on ASTM D7869

Mode	Mechanism attributed	Relevant stress factors
Solder-bond failure leading to open circuit	Insufficiently bonded solder joint at bus ribbon, believed compromised during soldering of junction box, joule heating in the conductors	Mechanical and thermomechanical stress on conductors. Applied light leading to joule heating in the conductors
Light-induced degradation	a) UV degradation of cell fronts, e.g. by loss of hydrogen passivation in modules using UV-transmissive EVA, leading primarily to I_{sc} and V_{oc} loss b) Light and elevated temperature-induced degradation, tentatively associated with H complexing in the Si cell	a) UV component of full-spectrum light applied b) Elevated temperature and light
Cracking of backsheet	Possible hydrolytic and oxidative reactions causing loss of volatile compounds embrittlement, shrinkage, and tensile stress	Heat, humidity, mechanical, and thermomechanical stress
Corrosion, ion migration	Ion formation and migration of ionic species facilitated by humidity and electric field	Heat, humidity, full-spectrum light, and system voltage bias
Potential-induced degradation	Ion formation and migration facilitated by humidity, electric field	Heat, humidity, and system voltage bias, modulated by applied light
Cell cracks	Crack progression from tensile stresses	Mechanical pressure, thermomechanical stress

An examination of the cracking of the polymer C backsheet is covered in more detail in Figure 18 [55]. It could clearly be seen that the degradation mode involves shrinkage of the backsheet. This is evident in the delamination starting at the corners (see Figure 18a)) and increasing separation of the encapsulant from the glass edge (as in Figure 18b)). The increase in displacement of the glass from the backsheet edge was about 0,046 mm/week in the four-cell mini-module. Cracking is detected at 19 weeks of C-AST as seen in Figure 18c). Examples of this material failing in the field within five years are shown in Figure 8b), indicating an acceleration of around 14 for this failure mechanism by the test protocol applied. Testing on



- a) Delamination at module edge seen at week 8;
 b) Shrinkage of backsheet offset from glass edge of about 1 mm shown at week 22 on the right (encircled) compared to the initial state shown to the left; and
 c) Resulting cracking at backsheet over interconnect ribbons.

Figure 18 – Shrinkage of polymer C backsheet leading to delamination and cracking

**Table 16 – Combined accelerated stress test
(Tropical 24 h ASTM D7869-based sequence)**

Sequential/ combined	Stress factor A	Stress factor B	Stress factor C	Stress factor D	Stress factor E	Combined stress effect(s)
	Rain	Freeze	V_{sys} bias	Full spectrum light	Mechanical pressure	
Material						
Coupon						
Mini-module	40 °C / 85 % Rain spray	-20 °C	90 °C module temperature / 28 % RH / V_{sys}	1,9 suns max. (other conditions per stress factor C)	+1 000 Pa and + 2 400 Pa equivalent	Backsheet: shrinkage cracking yellowing Cell: UVD & LeTID PID Solder-bond failure at: cell, tab, junction box Cell crack growth Corrosion
Module						
Sequential/Combined: (A (C + D + E) B + E [(C + D) A] x 4) x n cycles; cycle = 1 d						

module-representative samples of sufficient size and adhered to the superstructure (i.e. glass) provides the constraint of placing the backsheet in a state of tension, which produces cracking as the material shrinks. Some polymer C compounds are reported to change physical properties and shrink with loss of water and other volatile compounds [56-58]. Further, the additional stress associated with the deformation around interconnect ribbons where cracking nucleates appears to be important for representing the failure as it does on a module.

The degradation modes seen in the first experiment through C-AST are summarized in Table 15. These are associated with weaknesses of the module construction or designs that could be simultaneously evaluated by the test. These modes include degradation by UV radiation associated with loss of passivating hydrogen from the front of the cell that reduces cell efficiency in modules constructed with the UV-passing EVA [59], solder-bond failure, cell crack growth, interconnect corrosion, encapsulant discoloration, and backsheet discoloration. PID could be seen by reduced electroluminescence emission at the cell edges closest to the specimen periphery (where an Al foil was conductively adhered to the edge of the module face to act as a pseudo frame), which can be seen in Figure 18a) [55]. A summary of the sample type used, stress factors, and their sequence and combination, along with resulting degradation modes seen for the modules in the study, is given in Table 17.

7.2 Combined-accelerated stress testing for multiple environments

Testing to account for specific climates (e.g. tropical, continental, arctic) and all seasons is of interest. A module that may perform well in a tropical environment may not perform well in a cold, polar environment if there are components that, either when new or after aging, become stiff and brittle in cold temperatures. Hydrolytic reactions that may occur during a monsoon season may only manifest in failure in a following hot and dry season. Testing may therefore preferably include conditions representing the various seasons or climatic conditions. Furthermore, some mechanisms, such as LID associated with the boron-oxygen complex can be distinguished at moderate temperatures under illumination, thus requiring a period of stress testing under lower temperatures in addition to the higher-temperature tests. Modulus of elasticity of polymeric materials such as EVA are over an order-of-magnitude higher at -30 °C compared to room temperature, requiring understanding of the mechanical behaviour and

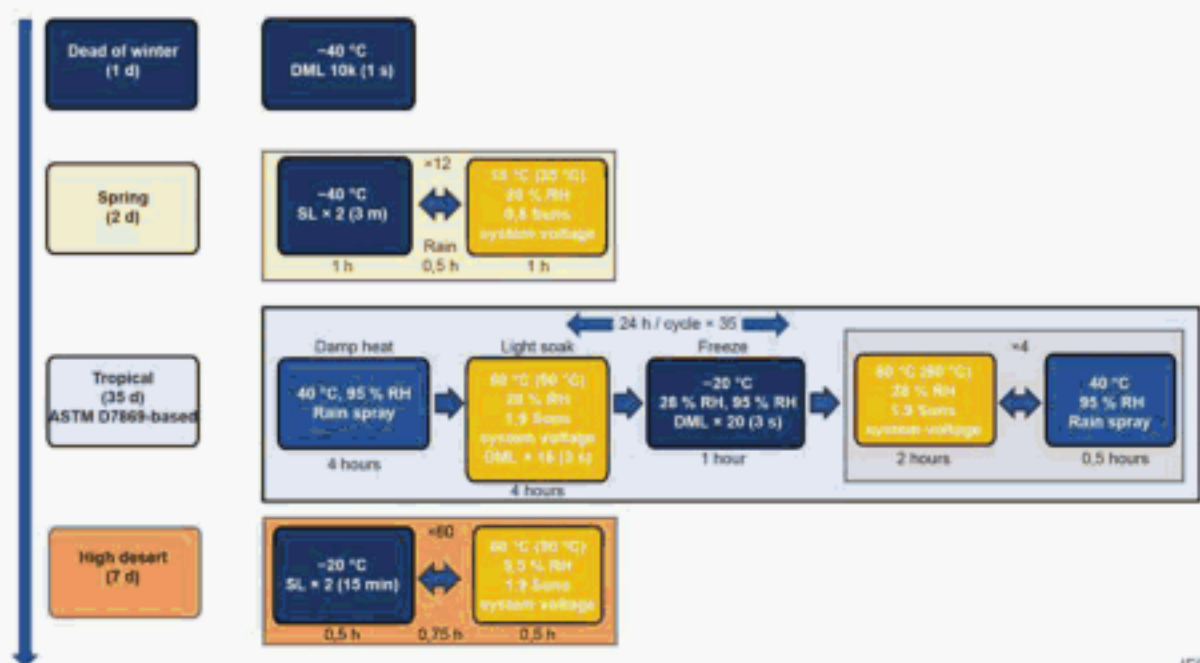
potential failure modes of the module under the wide range of potential field temperature conditions.

In view of the need to better represent the various seasons and climates with the combination of stress factors seen, climate sequences were devised as follows.

- Dead of winter: Simulating conditions found in a continental climate in winter, with application of simulated wind load at very low temperature using DML, without light.
- Spring: Simulating snow loads with application of SML and condensing humidity with freezes followed by thaw cycles with moderate light levels.
- Tropical: The modified ASTM D7869 protocol developed for acceleration in the Florida environment, including with higher sample temperature, V_{sys} stress, DML level stress, and cyclic freezes. This protocol was introduced in 7.1.
- High desert: Providing conditions for representation of a dry climate with hot days and cold nights.

The details of the climate sequences that were developed and cyclically applied are shown in Figure 19 [60]; however, the details of the test continue to be refined.

Two mini-modules with a polymer B outer-layer backsheet on the market discussed in 5.5 that cracked in the field (i.e. Figure 8d)) were examined in a multiple-environment C-AST sequence under development that is similar to, but not identical to, that shown in Figure 19. One mini-module underwent 12 weeks and another underwent 24 weeks of the Tropical sequence shown in Figure 17 and also shown within Figure 19. No degradation in the polymer B could be observed in either sample afterwards. The relatively short sequences of Dead of Winter and Spring (without spray, in this particular running of the test) were next applied, after which no failure could be observed in either sample. However, the backsheet in both samples cracked when subsequently performing the High Desert sequence as illustrated in Figure 20, see also Table 17.



IEC

Module temperature, when different from chamber air temperature, is shown in parentheses. Ramp stages of light, temperature and humidity and their times are not necessarily included, and time shown is sometimes rounded to the next-higher integer unit.

Figure 19 – Multiple-environment C-AST sequence

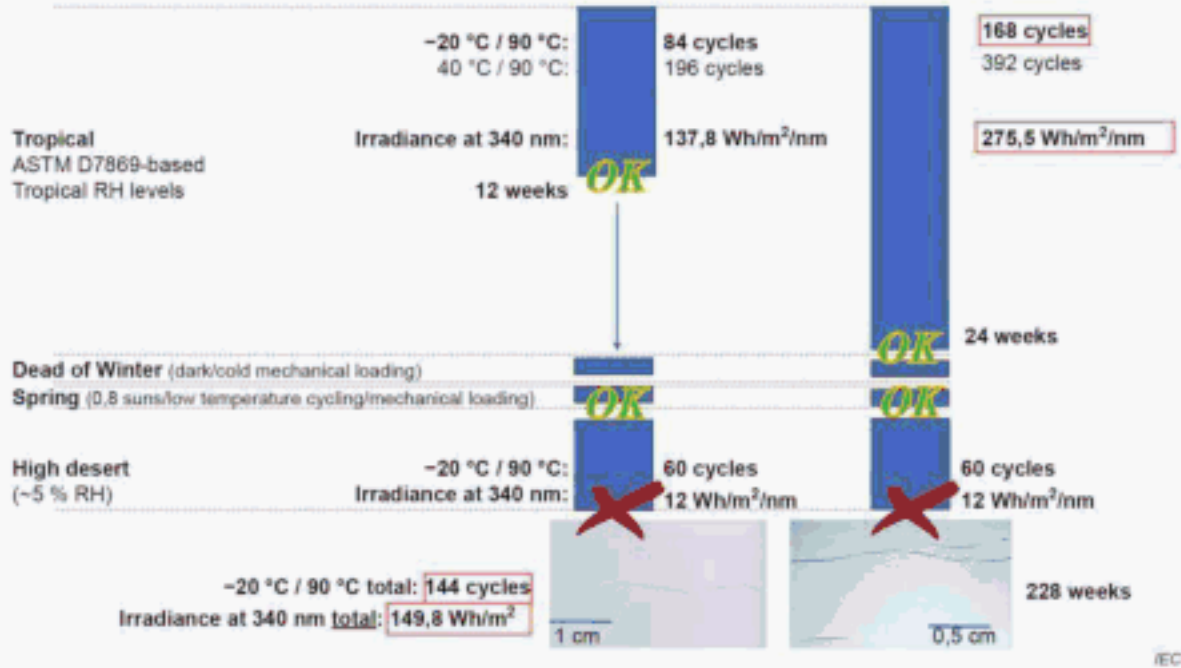


Figure 20 – Failure of two mini-modules with a polymer B outer-layer backsheet type undergoing different multiple-environment C-AST sequences

Table 17 – Multiple-environment combined accelerated stress test

Sequential/ combined	Stress factor A	Stress factor B	Stress factor C	Stress factor D	Combined stress effect(s)
	Tropical	Dead of winter	Winter to spring	High desert	
Material					
Coupon					
Mini-module	Table 16 – Combined-accelerated stress test (tropical 24 h ASTM D7869-based sequence) x n cycles or days	- 40 °C module temperature, DML 10 K cycles, 1 d	(20% / RH 35 °C module temperature 0,8 suns 1/sys -40 °C, SML x 2) x 12, 2 d	(- 20 °C / SML x 2 90 °C module temperature, 5 % RH 1,9 suns SML x 2) x 60, 7 d	Table 16 – Combined-accelerated stress test (tropical 24 h ASTM D7869-based sequence) degradation modes, plus a polymer B-type backsheet failure
Module					
Sequential/Combined: (A B C D) x n					

The mini-module with polymer B that underwent 12 weeks in the Tropical test that cracked after the subsequently applied High Desert sequence had a total of 144 thermal cycles between - 20 °C and 90 °C and UV radiation exposure of 149,8 Wh/m² at 340 nm on the rear of the module applied, which is significantly fewer thermal cycles and less light than the other sample underwent within the 24 weeks of the Tropical sequence, 168 cycles and 275,52 Wh/m² at 340 nm, without failing. This suggests that humidity, thermal cycles, and light at high temperature in the Tropical sequence alone is not optimum to show the backsheet weakness considering the effect of the subsequent dry High Desert applied for a short time that precipitated failure (see Figure 20).

A summary of the sample type used, stress factors, and their sequence and combination, along with resulting degradation modes seen for the modules in the study, is given in Table A.1.

8 Future directions

Many researchers around the world studying PV module reliability are converging to the understanding that single-factor and steady-state accelerated stress tests are insufficient to address the various degradation modes that can exist in PV modules. Progress has been made in the PV reliability community to:

- a) combine the stress factors of the natural environment for achieving more representative accelerated tests, and
- b) understand how stress factors work in sequence and in combination to reproduce failures seen in the field. Annex A gives an overview of degradation modes and causal stress factors working in combination.

Sequential tests are being incorporated into standardized tests. IEC 61215-1:2016 contains a brief UV precondition test of 15 kWh/m², followed by thermal cycling (50 cycles) and humidity-freeze (10 cycles) to test for the mechanisms whereby:

- 1) UV radiation causes failure of adhesion, and
- 2) humidity-freeze testing leads to moisture ingress through those interfaces and delamination as moisture precipitates out to weaken adhesive bonds.

It is anticipated that the future edition of IEC 61215-1 will add cyclic (dynamic) mechanical loading that is described in IEC TS 62782 before the thermal cycling test in the above-described sequence for further mechanical loading that is followed by thermal cycling and humidity freeze. IEC 61730-2:2016 contains a number of stress sequences, including DH testing of 200 h, UV radiation testing with 60 kWh/m², humidity-freeze (10 cycles), followed by a second repetition of this UV radiation and humidity-freeze testing. Results of such test sequences showing field validated failure modes were however not available for this report.

Concepts have been reviewed for sequential and combined accelerated stress testing for reproducing degradation and failure modes seen in the field. Degradation modes detected in these sequential and combined accelerated stress tests can be visualized on the failure tree diagram, developed by the INFINITY project [61, 62]. Although blank areas remain in many parts of the diagrams, testing of various susceptible samples would continue to complete the areas. Although all degradation modes (and their corresponding stress combinations that would elucidate them) could not be covered in detail, application of the framework shown in Figure 1 with the three axes that show incrementally the progression toward comprehensiveness—sample, factors, and combination in the testing—will achieve an understanding of potential degradation modes in given modules and increased confidence in the durability. With this framework, the module designer is guided on how to best develop testing protocols with full awareness of how each test type fits the needs in the various phases of product development to gain confidence in the final module construction.

In the combined approach, we seek to include the effects of the cyclic and sequential nature of the stresses in the natural environment such as diurnal and seasonal cycling. For some degradation modes, as with the example of PID rate that is influenced by humidity, voltage, and light, there are often multiple factors that exist together in the natural environment that need to appear together in tests to most accurately forecast the extent that the degradation mode will be seen in the field. When any new, uncomprehended degradation mode is observed, or the rate of the degradation is faster than anticipated, we require a more focused study on the underlying mechanism, including an analysis of the root causes and determination of the acceleration factors.

Presently, commercial environmental test chambers for PV modules are usually optimized for single- or two-factor tests. However, many are extending use of environmental chambers to perform sequential and cyclic sequential testing to better characterize some potential failure modes not well characterized by steady-state tests. We will greatly benefit from further development of toolsets to achieve the comprehensiveness in the samples tested (including for

multiple full-size modules) in addition to the combination of applied stresses for better representation of the stresses in the natural environment and realistic degradation results. We will be well served by further understanding and optimizing sequential and combined stress-testing methodologies so that risk can be reduced and costly overdesign avoided. We also anticipate the number of factor-specific tests in parallel can be reduced significantly when:

- c) samples are made more representative of the final module (if not using the module product itself),
- d) the number of field-representative stress factors included in testing is maximized, and
- e) the stress factors are combined as they are in the natural environment.

When a well-designed multi-factor test performed on modules that includes the various stress factors of the natural environment in combination is obtained, detection of the majority of PV module degradation modes (both known and previously undetected) is anticipated, thus reducing risk with fewer samples and at reduced cost.

Annex A

(informative)

Overview of degradation modes and causal stress factors

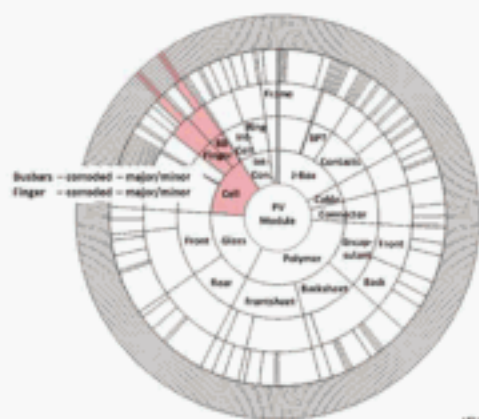
The International Photovoltaic Quality Assurance Task Force (PVQAT) Task Group 3, which holds periodic meetings with international PV industry experts, deals with PV module reliability and focuses on the stress factors of temperature, humidity, and voltage. As shown in Table A.1, the group summarized stress factors that can work individually or collectively to effect the listed degradation or failure modes. The table is not comprehensive as to cover every situation. Furthermore, the scope does not include the weaknesses in materials or manufacturing process that may increase the rate or prevalence of the degradation and failure modes discussed. Temperature, when meaning that high temperature or low temperature can bring about the degradation, is referred to only as temperature.

Table A.1 – Degradation modes and potential stress factors that can lead to their manifestation

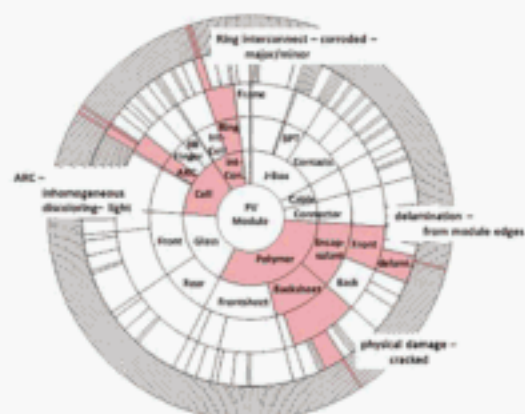
Potential-induced degradation-shunting mode	LID (various types, including UV degradation of cells)	Solder and ribbon failure (and any resulting arcing)	Ag grid-finger delamination from cell	Bypass-diode failure
(PID-s)				
System voltage	Light	High temperature	High temperature	High temperature
High temperature	Temperature	Temperature cycling	Humidity (with EVA acidity)	Shading (current, turn-on)
Humidity	Injected carriers (current)	Mechanical stress	Temperature cycling	Broken cells (current, turn-on)
Light		Humidity (with EVA and solder flux acidity)	Mechanical stress	Electrical discharge
Stress history		Current/bias		
Cell junction potential (bias or load)				
Injected carriers (current)				
Delamination (and any resulting ground faults)	Cell cracks	Corrosion	Burns and breaks in package	Glass breakage (and resulting ground faults)
Humidity	Mechanical stress	Voltage (in cells)	Bypass-diode failure (and its respective causes)	Bypass-diode failure (and its respective causes)
Light	Temperature cycling	High temperature	Solder-fatigue failure (and respective causes)	Solder-fatigue failure (and respective causes)
Voltage (internal)	Temperature	Humidity (with EVA and solder flux acidity)	System voltage	Projectiles
Temperature		System voltage		Mechanical loading
Mechanical loading (including cell cracks)		Acid/base/corrosive chemicals		
System voltage		Voltage (in cells)		
Temperature cycling				
discoloration Glass	corrosion/permanent soiling	Polymeric mechanical failure, creep, cracking (and any resulting ground faults)		
High temperature	Humidity	Acid (including in EVA)		
Light	Voltage: V_{sys} can attract species, carriers can oxidize or reduce	Light		
Humidity	Surface energy	Temperature		
Acid/base/corrosive chemicals	Acid/base/corrosive chemicals (base dissolves glass, acid, dissolves Na out of glass)	Mechanical stress (both intrinsic built-in stress and external loads)		
	Soils, aerosols, calcium deposits	Humidity		
	Wind/blowing particles: abrasion	Temperature cycling		

Annex B (informative)

Failure modes plotted on a failure tree diagram for selected clauses in this document



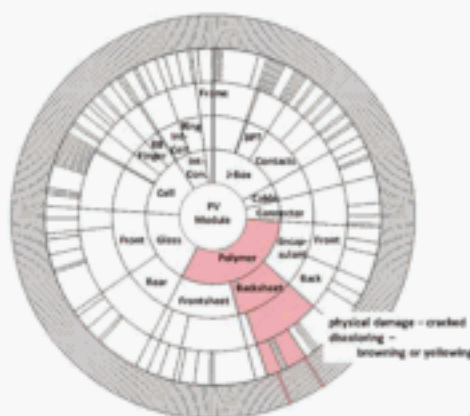
IEC



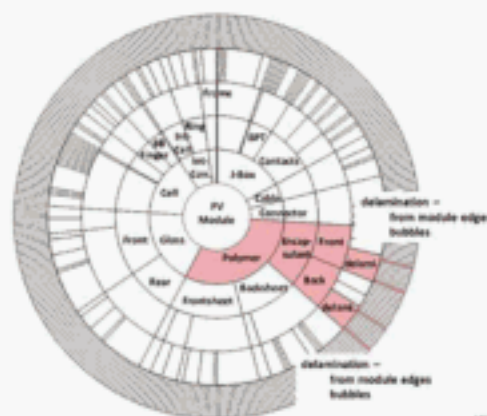
IEC

a) Extended damp heat and UV radiation, sequential/combined testing with damp-heat thermal cycling and UV radiation, and consideration of interaction of damp heat and of UV radiation

b) Test-to-failure sequential test protocol



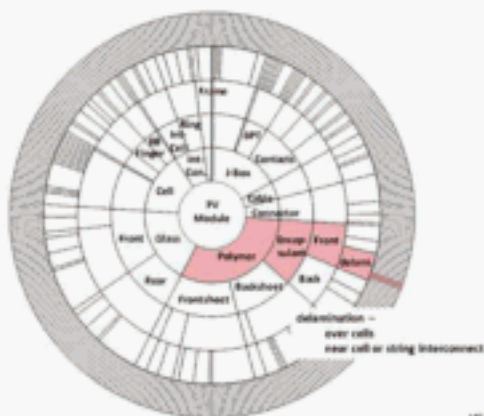
IEC



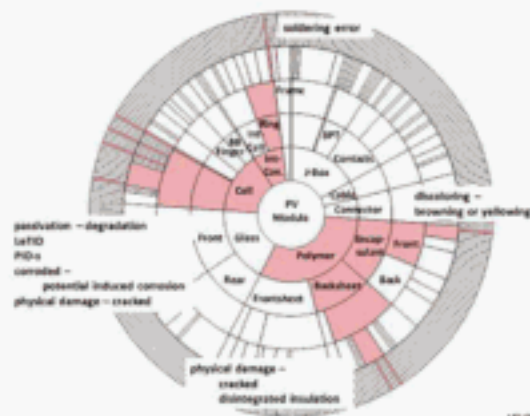
IEC

c) Module accelerated stress tests (MAST #1- #3)

d) UV irradiation with DML-TC-HF sequential test in a glass-glass module



IEC



IEC

e) DH - negative system bias stress sequential test

f) Combined accelerated stress test (24 h sequence)

Annex C
(informative)

**Summary table of sequential and combined testing:
Samples, factors, combination, and stress test results**

This Annex is a summary of sequential and combined test studies included in this document provided in one table: Table C.1.

Table C.1 – Table summarizing sequential and combined stress testing

Extended damp heat and UV radiation			
Sequential/ combined	Stress factor A	Stress factor B	Combined stress effect(s)
	DH	UV+DH	
Material			
Coupon			
Mini-module			
Module	85 °C/85 % RH 2 000 h	200 W/m ² UV-A, 85 °C module temperature, 2 000 h	Degradation of <i>I_{sc}</i> and <i>FF</i> in better proportion to field, toward field-relevant levels of humidity after UV exposure.
Sequential / Combined: A B			

Sequential/combined testing with damp-heat thermal cycling and UV radiation				
Sequential/ combined	Stress factor A	Stress factor B	Stress factor C	Combined stress effect(s)
	DH	TC	DH/UV	
Material				
Coupon				
Mini-module				
Module	85 °C/ 85 % RH 1 000 h or 500 h	–40 °C/ 85 °C 100 cycles	200 W/m ² UV-A, 85 °C module temperature, 500 h	Degradation of <i>I_{sc}</i> and <i>FF</i> in proportion to field, toward field- relevant levels of humidity ingress with use of UV exposure
Sequential/Combined: A B C [A B C] × n				
The stress sequence (A–C) is repeated cyclically; however, Stress Factor A (DH) time is reduced to 500 h after the first time.				

UV radiation and damp-heat interaction			
Sequential/ combined	Stress factor A	Stress factor B	Combined stress effect(s)
	UV	DH	
Material			
Coupon			
Mini-module	1,5 suns UV, 90 °C module temperature 1 500 h to 4 000 h	85 °C/ 85 % RH 1 500 h	UV radiation activates appearance of acetic acid in subsequent DH, causing increased contact resistance of grid fingers to silicon
Module			
Sequential: A B			

Test-to-failure – Sequential test protocol				
Sequential/ combined	Stress factor A	Stress factor B	Stress factor C	Combined stress effect(s)
	DH / V_{sys} bias (+) and (-)	TC with application of I_{sc}	Cyclic application of stress factors A and B	
Material				
Coupon				
Mini-module				
Module	85 °C/85 % RH, +600 V or -600 V, 1 000 h	-40 °C/ 85 °C, I_{sc} , 200 cycles	TC with application of I_{sc}	Backsheet cracking, corrosion, delamination, PID, solder-bond failure, antireflective-coating degradation
Sequential/Combined: A, B; C = [A B] × n				

Module accelerated stress test 1 (MAST #1)				
Sequential/ combined	Stress factor A	Stress factor B	Stress factor C	Combined stress effect(s)
	DH	UV	TC	
Material				
Coupon				
Mini-module	85 °C / 85 % 1 000 h	70 °C or 75 °C module temperature, 65 W/m ² (300 nm to 400 nm) 542 h	TC (-40 °C/ 85 °C)	Backsheet cracking
Module				
Sequential: A B [C B] × n				

Module accelerated stress test 2 (MAST #2)			
Sequential/ combined	Stress factor A	Stress factor B	Combined stress effect(s)
	DH	TC	
Material			
Coupon			
Mini-module	85 °C / 85 % RH 1 000 h	3 x TC 200 (-40 °C/ 85 °C)	Backsheet cracking (polymer C)
Module			
Sequential: A B			

Module accelerated stress test 3 (MAST #3)			
Sequential/ combined	Stress factor A	Stress factor B	Combined stress effect(s)
	UV + T	Water spray	
Material			
Coupon			
Mini-module	90 °C, 123 W/m ² (300 nm to 400 nm) 102 min	18 min (in the dark)	Backsheet yellowing Backsheet cracking
Module			
Sequential: [A B] × 1 500 cycles			

SML-TC-HF sequential test				
Sequential/ combined	Stress factor A	Stress factor B	Stress factor C	Combined stress effect(s)
	SML	TC	HF	
Material				
Coupon				
Mini-module				
Module	2 400 Pa (IEC 61215-2, modified)	TC (IEC 61215-2, modified)	HF (IEC 61215-2, modified)	A greater drop in the performance parameters after TC and HF test. Cell cracking
Sequential: A B C A C				

UV irradiation under high-temperature conditions		
Sequential/ combined	Stress factor A	Combined stress effect(s)
	UV + T	
Material		
Coupon		
Mini-module		
Module	180 W/m ² at 65 °C	Delamination
Stress factor A: UV radiation with elevated temperature		

UV irradiation with TC stress			
Sequential/ combined	Stress factor A	Stress factor B	Combined stress effect(s)
	UV + T	TC	
Material			
Coupon			
Mini-module			
Module	180 W/m ² at 75 °C module temperature, 1 h	-20 °C / +75 °C, 1 h dwells	Delamination (starting after 75 cycles, significant at 125 cycles)
Combined: A + B			

UV irradiation with DML-TC-HF sequential test					
Sequential/ combined	Stress factor A	Stress factor B	Stress factor C	Stress factor D	Combined stress effect(s)
	UV	DML	TC	HF	
Material					
Coupon					
Mini-module	UV-A (65 W/m ²) 70 °C) 1 000 h	±1 500 Pa, 0,167 Hz, room temperature 2 x 1 000 cycles	IEC 61215-2 200 cycles	IEC 61215-2 30 cycles	Delamination in a glass-glass module
Module					
Sequential: A B C D B					

DH – Negative system bias stress sequential test			
Sequential/ combined	Stress factor A	Stress factor B	Combined stress effect(s)
	DH	DH / V _{sys} (-)	
Material			
Coupon			
Mini-module	85 °C / 85 % RH 1 000 h	72 °C / 95 % RH, -1 000 V	Delamination: Stress factor B 110 h, small; 247 h, significant
Module	85 °C / 85 % RH 1 000 h	72 °C / 95 % RH, -1 000 V	Significant delamination: Stress factor B 156 h
Sequential A B			

UV irradiation – negative system bias stress combined test			
Sequential/ combined	Stress factor A	Stress factor B	Combined stress effect(s)
	DH	DH / V _{sys} bias (-)	
Material			
Coupon			
Mini-module			
Module	UV-A: 5 W/m ²	60 °C / 85 % RH module surface / -1 000 V, 96 h	Elimination or slowing of PID-shunting
Combined: A + B			

Bending load test at various temperatures			
Sequential/ combined	Stress factor A	Stress factor B	Combined stress effect(s)
	Bending load	Temperature	
Material			
Coupon			
Mini-module	500 N, -30 K cycles	-20 °C, +25 °C, and +80 °C	Low temperature: Cell cracking; High temperature: Ribbon fracture
Module			
Combined: A + B			

Combined-accelerated stress test (Tropical 24 h ASTM D7869-based sequence)						
Sequential/ combined	Stress factor A	Stress factor B	Stress factor C	Stress factor D	Stress factor E	Combined stress effect(s)
	Rain	Freeze	V_{sys} bias	Full-spectrum light	Mechanical pressure	
Material						
Coupon						
Mini-module	40 °C / 85 % Rain spray	-20 °C	90 °C module temperature / 28 % RH / V_{sys}	1,9 suns max (other conditions per Stress Factor C)	+1 000 Pa and + 2 400 Pa equivalent	Backsheet: shrinkage cracking yellowing Cell: UVD & LeTID PID Solder-bond failure at: cell, tab, junction box Cell crack growth Corrosion
Module						
Sequential/Combined: (A (C + D + E) B + E [(C + D) A] x 4) x n cycles; cycle = 1 d						

Multiple-environment combined-accelerated stress test					
Sequential/ combined	Stress factor A	Stress factor B	Stress factor C	Stress factor D	Combined stress effect(s)
	Tropical	Dead of winter	Winter to spring	High desert	
Material					
Coupon					
Mini-Module	Combined- accelerated stress test (tropical 24 h ASTM D7869- based sequence) x n cycles or days	- 40 °C module temperature, DML 10 K cycles, 1 d	(20% / RH 35 °C module temperature temperature V_{sys} = 40 °C, SML x 2) x 12, 2 d	(- 20 °C / SML x 2 90 °C module temperature, 5 % RH 1,9 suns SML x 2) x 60, 7 d	Combined- accelerated stress test (tropical 24 h ASTM D7869 -based sequence) degradation modes, plus a polymer B-type backsheet failure
Module					
Sequential/Combined: (A B C D) x n					

Bibliography

- [1] KOEHL, M., S. HOFFMANN AND K.-A. WEISS 2014. Combined Stress Factor Testing of PV Modules. In Proceedings of the 29th European Photovoltaic Solar Energy Conference and Exhibition, 2014.
- [2] JORDAN, D. C., J. H. WOHLGEMUTH AND S. R. KURTZ Technology and climate trends in PV module degradation. In Proceedings of the 27th European Photovoltaic Solar Energy Conference and Exhibition, 2012, pp 3118-3124.
- [3] WITTECK, R., B. VEITH-WOLF, H. SCHULTE-HUXEL, A. MORLIER, et al. UV-induced degradation of PERC solar modules with UV-transparent encapsulation materials. Progress in Photovoltaics: Research and Applications, 2017, 25(6), pp 409-416.
- [4] MILLER, D. C., E. ANNIGONI, A. BALLION, J. G. BOKRIA, et al. Degradation in PV encapsulation transmittance: an interlaboratory study towards a climate-specific test. In Photovoltaic Specialist Conference (PVSC), 42nd, IEEE, 2015, pp 1-6.
- [5] COYLE, D. J. Life prediction for CIGS solar modules part 1: modeling moisture ingress and degradation. Progress in Photovoltaics: Research and Applications, 2013, 21(2), pp 156-172.
- [6] KEMPE, M. D., D. PANCHAGADE, M. O. REESE AND A. A. DAMERON Modeling moisture ingress through polyisobutylene-based edge-seals. Progress in Photovoltaics: Research and Applications, 2015, 23(5), pp 570-581.
- [7] KEMPE, M. D. AND J. H. WOHLGEMUTH. Evaluation of temperature and humidity on PV module component degradation. In Photovoltaic Specialists Conference (PVSC), 39th, IEEE, 2013, pp 0120-0125.
- [8] SHIODA, T. Acetic acid production rate in EVA encapsulant and its influence on performance of PV modules. In 2nd Atlas/NIST PV Materials Durability Workshop. Gaithersburg, 2013.
- [9] NGO, T., Y. HETA, T. DOI AND A. MASUDA Effects of UV on power degradation of photovoltaic modules in combined acceleration tests. Japanese Journal of Applied Physics, 2016, 55(5), 052301.
- [10] OSTERWALD, C. R. Terrestrial Photovoltaic Module Accelerated Test-To-Failure Protocol. NREL Technical Report, NREL/TP-520-42893, 2008.
- [11] HACKE, P., K. TERWILLIGER, S. GLICK, D. TRUDELL, et al. Test-to-failure of crystalline silicon modules. In Photovoltaic Specialists Conference (PVSC), 35th, IEEE, 2010, pp 000244-000250.
- [12] HACKE, P., K. TERWILLIGER, S. GLICK, R. SMITH, et al. Application of the terrestrial photovoltaic module accelerated test-to-failure protocol. In Photovoltaic Specialist Conference (PVSC), 40th., IEEE, 2014, pp 0930-0936.
- [13] MASUDA, A., C. YAMAMOTO, N. UCHIYAMA, K. UENO, et al. Sequential and combined acceleration tests for crystalline Si photovoltaic modules. Japanese Journal of Applied Physics, 2016, 55(4S), 04ES10.
- [14] TAMIZHMANI, G. Long-term sequential testing (LST) of PV modules. In 2012 PV Module Reliability Workshop. Golden, 2012.

- [15] GAMBOGI, W., T. FELDER, B. L. YU, S. MACMASTER, et al. Module Accelerated Stress Testing and Comparison to Field Performance. In NREL Photovoltaic Reliability Workshop. Lakewood, CO, 2017, p 344.
- [16] GAMBOGI, W., T. FELDER, S. MACMASTER, K. ROY-CHOUDHURY, et al. Sequential Stress Testing to Predict Photovoltaic Module Durability. IEEE 7th World Conference on Photovoltaic Energy Conversion (WCPEC)(A Joint Conference of 45th IEEE PVSC, 28th PVSEC & 34th EU PVSEC), 2018, pp 1593-1596.
- [17] RUMMENS, F. 2012. High Speed Automated Production of Durable PV Modules: The Contribution of Cost Effective Adhesive Integrated and Weldable Backsheets. In Proceedings of the 2nd Polymer Apps in PV, Leipzig, 12-13 March 2012.
- [18] CHOUDHURY, K. R., W. GAMBOGI, T.-J. TROUT AND R. DESHARNAIS 2018. Backsheet Degradation in Accelerated Sequential Testing of Full-size Commercial Modules. In 2018 NREL PV Reliability Workshop, Lakewood, CO, 2018.
- [19] GAMBOGI, W., T. FELDER, K. R. CHOUDHURY, S. MACMASTER, et al. Accelerated Testing Using Multiple Sequential Stresses and Comparison to Field Performance. In NREL PV Reliability Workshop. Lakewood, CO 2018.
- [20] GAMBOGI, W., J. KOPCHICK, T. FELDER, S. MACMASTER, et al. Development of Accelerated Tests Based on Analysis of Fielded Modules. In 3rd Atlas/NIST Workshop on Photovoltaic Materials Durability. Gaithersburg MD, 2015.
- [21] GAMBOGI, W., S. MACMASTER, B.-L. YU, T. FELDER, et al. Sequential Testing That Better Predicts Field Performance. In 4th Atlas-NIST Workshop on PV Materials Durability. Gaithersburg MD, 2017.
- [22] SEIGNEUR, H., E. SCHNELLER, J. LINCOLN AND A. M. GABOR 2018. Cyclic Mechanical Loading of Solar Panels – A Field Experiment. In Proceedings of the 7th World Conference on Photovoltaic Energy Conversion (WCPEC-7), 2018, IEEE, pp 3810-3814.
- [23] SPATARU, S., P. HACKE AND D. SERA. In-situ measurement of power loss for crystalline silicon modules undergoing thermal cycling and mechanical loading stress testing. In Workshop Crystalline Silicon Solar Cells Modules, Materials Processes, Keystone, CO, USA. 2015.
- [24] BUERHOP, C. The Relevance of Controlling the Quality of PV-Systems. In 2018 NREL PV Reliability Workshop. Lakewood, CO, 2018.
- [25] ROWELL, M. W., S. G. DAROCZI, D. W. J. HARWOOD AND A. M. GABOR 2018. The Effect of Laminate Construction and Temperature Cycling on the Fracture Strength and Performance of Encapsulated Solar Cells. In Proceedings of the 7th World Conference on Photovoltaic Energy Conversion (WCPEC-7), Waikoloa Village, June 10–15, 2018, IEEE, pp 3927-3931.
- [26] WOHLGEMUTH, J. H., P. HACKE, N. BOSCO, D. C. MILLER, et al. Assessing the causes of encapsulant delamination in PV modules. In Photovoltaic Specialist Conference (PVSC), 2017 IEEE 44th. IEEE, 2017, pp 1-6.
- [27] MATSUDA, K., T. WATANABE, K. SAKAGUCHI, M. YOSHIKAWA, et al. Microscopic degradation mechanisms in silicon photovoltaic module under long-term environmental exposure. Japanese Journal of Applied Physics, 2012, 51(10S), 10NF07.

- [28] Combined stress acceleration tests. In R&D of Characterization Technology of Solar Cells (FY2006-FY2009) Final Report, New Energy and Industrial Technology Development Organization (in Japanese), 2010.
- [29] DHERE, N. G., N. R. RARAVIKAR, A. MIKONOWICZ AND C. CORDING. Effect of glass Na content on adhesional strength of PV modules. In Photovoltaic Specialists Conference, 2002. Conference Record of the Twenty-Ninth IEEE, 2002, pp 231-234.
- [30] HACKE, P., M. KEMPE, J. WOHLGEMUTH, J. LI, et al. 2016. Potential-Induced Degradation-Delamination Mode in Crystalline Silicon Modules. In Proceedings of the 2016 Workshop on Crystalline Silicon Solar Cells and Modules: Materials and Processes, Vail, CO2016 NREL.
- [31] HACKE, P., M. KEMPE, K. TERWILLIGER, S. GLICK, et al. 2010. Characterization of multicrystalline silicon modules with system bias voltage applied in damp heat. In Proceedings of the 25th EUPVSEC and Exhibition/5th WCPEC, 2010.
- [32] LI, J., Y.-C. SHEN, P. HACKE AND M. KEMPE Electrochemical Mechanisms of Leakage-Current-Enhanced Delamination and Corrosion in Si Photovoltaic Modules Solar Energy Materials and Solar Cells, Vol. 18, 2018, pp 273-279
- [33] BOSCO, N., P. HACKE, S. KURTZ, J. TRACY, et al. 2017. Adhesion Degradation of the Metallization-Encapsulant Interface. In Proceedings of the 33rd European Photovoltaic Solar Energy Conference and Exhibition, 2017, pp 1336 – 1339.
- [34] MON, G., L. WEN, R. ROSS AND D. ADENT. Effects of temperature and moisture on module leakage currents. In Photovoltaic Specialist Conference (PVSC), 18th, IEEE, 1985, pp 1179-1185.
- [35] LUO, W., Y. S. KHOO, P. HACKE, V. NAUMANN, et al. Potential-induced degradation in photovoltaic modules: a critical review. Energy & Environmental Science, 2017, 10(1), pp 43-68.
- [36] SWANSON, R. M., D. DE CEUSTER, V. DESAI, D. H. ROSE, et al. Preventing harmful polarization of solar cells. US Patent US20060196535A1.
- [37] HACKE, P., K. TERWILLIGER, S. GLICK, G. TAMIZHMANI, et al. Interlaboratory study to determine repeatability of the damp-heat test method for potential-induced degradation and polarization in crystalline silicon photovoltaic modules. IEEE Journal of Photovoltaics, 2015, 5(1), pp 94-101.
- [38] LUO, W., P. HACKE, S. M. HSIAN, Y. WANG, et al. Investigation of the Impact of Illumination on the Polarization-Type Potential-Induced Degradation of Crystalline Silicon Photovoltaic Modules. IEEE Journal of Photovoltaics, 2018, 8(5), pp 1168-1173.
- [39] JONAI, S., T. TANAHASHI, H. SHIBATA AND A. MASUDA Effect of bias voltage application on potential-induced degradation for crystalline silicon photovoltaic modules. Japanese Journal of Applied Physics, 2018, 57(8S3), 08RG01.
- [40] SUZUKI, S., N. NISHIYAMA, S. YOSHINO, T. UJIRO, et al. Acceleration of potential-induced degradation by salt-mist preconditioning in crystalline silicon photovoltaic modules. Japanese Journal of Applied Physics, 2015, 54(8S1), 08KG08.
- [41] HACKE, P., P. BURTON, A. HENDRICKSON, S. SPATARU, et al. Effects of photovoltaic module soiling on glass surface resistance and potential-induced degradation. In Photovoltaic Specialist Conference (PVSC), 42nd, IEEE, 2015, pp 1-4.

- [42] LINDROOS, J. AND H. SAVIN Review of light-induced degradation in crystalline silicon solar cells. *Solar Energy Materials and Solar Cells*, 2016, 147, pp 115-126.
- [43] KERSTEN, F., P. ENGELHART, H.-C. PLOIGT, A. STEKOLNIKOV, et al. Degradation of multicrystalline silicon solar cells and modules after illumination at elevated temperature. *Solar Energy Materials and Solar Cells*, 2015, 142, pp 83-86.
- [44] RAMSPECK, K., S. ZIMMERMANN, H. NAGEL, A. METZ, et al. Light induced degradation of rear passivated mc-Si solar cells. In *Proc. 27th Eur. Photovolt. Sol. Energy Conf. Exhib.*, 2012, vol. 1, pp 861-865.
- [45] HERGUTH, A., G. SCHUBERT, M. KAES AND G. HAHN. A new approach to prevent the negative impact of the metastable defect in boron doped Cz silicon solar cells. In *Photovoltaic Energy Conversion, Conference Record of the 2006 IEEE 4th World Conference, IEEE*, 2006, vol. 1, pp 940-943.
- [46] NIEWELT, T., F. SCHINDLER, W. KWAPIL, R. EBERLE, et al. Understanding the light induced degradation at elevated temperatures: Similarities between multicrystalline and floatzone p-type silicon. *Progress in Photovoltaics: Research and Applications*, 2018, 26(8), pp 533-542.
- [47] CHEN, H., C. H. HSUEH, C. CHEN AND M. CHANG Accelerated Damp Heat Test Combining Current Stressor. 29th European Photovoltaic Solar Energy Conference and Exhibition, 2014, pp 3182 – 3185.
- [48] MICKIEWICZ, R., B. LI, D. DOBLE, T. CHRISTIAN, et al. Effect of encapsulation modulus on the response of PV modules to mechanical stress. In *Proceedings of the 26th European Photovoltaic Solar Energy Conference*. 2011, pp 3157 – 3161.
- [49] SUZUKI, S., T. DOI, A. MASUDA AND T. TANAHASHI Bending cyclic load test for crystalline silicon photovoltaic modules. *Japanese Journal of Applied Physics*, 2018, 57(2S2), 02CE05.
- [50] NICHOLS, M., J. BOISSEAU, L. PATTISON, D. CAMPBELL, et al. An improved accelerated weathering protocol to anticipate Florida exposure behavior of coatings. *Journal of Coatings Technology and Research*, 2013, 10(2), pp 153-173.
- [51] ASTM D7869 – 17 Standard Practice for Xenon Arc Exposure Test with Enhanced Light and Water Exposure for Transportation Coatings. ASTM International, 2017.
- [52] IEC 60721-2-1:2013, *Classification of environmental conditions – Part 2-1: Environmental conditions appearing in nature – Temperature and humidity*.
- [53] SPATARU, S., P. HACKE AND M. OWEN-BELLINI 2018. Combined-Accelerated Stress Testing System for Photovoltaic Modules. In *Proceedings of the 7th World Conference on Photovoltaic Energy Conversion (WCPEC-7)*, 2018, pp 3943-3948.
- [54] KURTZ, S., K. WHITFIELD, G. TAMIZHMANI, M. KOEHL, et al. Evaluation of high-temperature exposure of photovoltaic modules. *Progress in Photovoltaics: Research and Applications*, 2011, 19(8), pp 954-965.
- [55] OWEN-BELLINI, M., P. HACKE, M. KEMPE, D. MILLER, et al. 2018. Combined-Accelerated Stress Testing for Advanced Reliability Assessment of Photovoltaic Modules. In *Proceedings of the European Photovoltaic Solar Energy Conference and Exhibition (EU PVSEC)*, 2018, pp 1101 – 1105.

- [56] ACHHAMMER, B. G., F. W. REINHART AND G. M. KLINE Mechanism of the degradation of polyamides. *Journal of Applied Chemistry*, 1951, 1(7), pp 301-320.
- [57] MONSON, L., M. BRAUNWARTH AND C. EXTRAND Moisture absorption by various polyamides and their associated dimensional changes. *Journal of Applied Polymer Science*, 2008, 107(1), pp 355-363.
- [58] GERBIG, S. Polyamide Moisture Absorption | Relative Dimensional Change of Various Nylon Products. UL, 2014. <https://knowledge.ulprospector.com/1390/polyamide-moisture-absorption>, accessed Nov. 2019.
- [59] ROBERT WITTECK, H. S.-H., BORIS VEITH-WOLF, MALTE RUBEN VOGT, FABIAN KIEFER, MARC KÖNTGES, ROBBY PEIBST, ROLF BRENDEL 2017. Reducing UV induced degradation losses of solar modules with c-Si solar cells featuring dielectric passivation layers. In *Photovoltaic Specialists Conference*, 44th, IEEE, 2017, pp 1366-1370.
- [60] HACKE, P. Development of Combined and Sequential Accelerated Stress Testing for Derisking Photovoltaic Modules. NREL Technical Report NREL/PR-5K00-73984, 2019.
- [61] HALWACHS, M., K. A. BERGER, M. SCHWARK, R. EBNER, et al. 2018. Trend analysis of PV module failure occurrence in different climate zones. In *Proceedings of the 35th European Photovoltaic Solar Energy Conference and Exhibition*, 2018.
- [62] ORESKI, G., A. OMAZIC, G. C. EDER, L. NEUMAIER, et al. PV Materials and Modules Developed for Certain Climatic Zones. In *35th European Photovoltaic Solar Energy Conference and Exhibition*, 2018.
-

